NASA-TM-111773

93179

LOW FREQUENCY WAVES IN THE PLASMA ENVIRONMENT AROUND THE SHUTTLE

Boris V. Vayner*, and Dale C. Ferguson♣

National Aeronautics and Space Administration

Lewis Research Center, Cleveland, Ohio 44135

As a part of the SAMPIE (The Solar Array Module Plasma Interaction Experiment) program, the Langmuir probe (LP) was employed to measure plasma characteristics during the flight of STS-62. The whole set of data could be divided into two parts : i) low frequency sweeps to determine voltage-current characteristics and to find the electron temperature and number density; ii) high frequency turbulence (HFT) data caused by electromagnetic noise around the Shuttle. Broadband noise was observed at 250-20,000 Hz frequencies. Measurements were performed in ram conditions; thus, it seems reasonable to believe that the influence of spacecraft operations on plasma parameters was minimized. It is shown that ion acoustic waves were observed, and two kinds of instabilities are suggested for explanation of the origin of these waves. According to the purposes of SAMPIE, samples of solar cells were placed in the cargo bay of the Shuttle, and high negative bias voltages were applied to them to initiate arcing between these cells and the surrounding plasma. The arcing onset was registered by special counters, and data were obtained that included the amplitudes of current, duration of each arc, and the number of arcs per one experiment. The LP data were analyzed for two different situations: with arcing and without arcing. Electrostatic noise spectra for both situations and a theoretical explanation of the observed features are presented in this paper.

---

*National Research Council-NASA Research Associate at Lewis Research Center.

♣Chief, Space Environment Effects Branch

Nomenclature

B	magnetic field strength
$D(f)$	observed spectrum
E, E	electrical field strength
f	frequency of plasma density fluctuations
f_{LH}	lower hybrid resonance frequency
F_i	ion gyrofrequency
I, i	LP current
k	wave vector
k_B	Boltzman constant
l	mean free path
L	spacecraft dimension
n_e	electron number density
n_g	number density of neutral molecules
n_i	ion number density
n(XX)	number density of species XX
N_{arc}	number of arcs per one experiment
p	neutral gas pressure
R	distance from spacecraft surface
t	time
T_e	electron temperature
T_g	initial water vapor temperature
T_i	ion temperature
U	LP output voltage
V	LP bias voltage
$\mathbf{V_D}$	plasma drift velocity
$\mathbf{V_s}$	spacecraft velocity
V_T	molecule thermal speed
W_s	IAW phase speed
x	vector of spatial coordinates
λ	IAW wave length
Θ	angle between the Earth magnetic field and the spacecraft velocity
σ	molecular cross section
τ_{exp}	duration of individual experiment with arcing
τ_{dwell}	duration of one dwell
$\omega_{1,2}$	ion plasma frequencies

Introduction

During the Space Shuttle flight STS-62 broadband electrostatic noise was observed at 250-20,000 Hz frequencies. The measurements were performed in ram conditions by the Langmuir probe (LP) flown as a part of the SAMPIE package .[1] The noise has almost a flat spectrum with a sharp decline near the lower hybrid resonance frequency f_{LH}, and the intensities range from 0.1 to 5 mV/m.[2] It should be noted that such noise was observed in ram conditions more than ten years ago,[3] but there is not yet a satisfactory explanation for the mechanism of generation. An investigation of plasma wave turbulence within a wide range of frequencies (from a few Hz to 200 kHz) was done by using the Plasma Diagnostic Package (PDP) during the SL-2 and STS-3 flights.[4,5] It was established that the noise is electrostatic, the highest intensities occured in the region downstream of the spacecraft, and the intensities increased considerably after water dumps .[6] Two different processes were considered in attempting to understand the generation (instability) of the plasma turbulence caused by a water release: the drift instability and the Ott-Farley instability caused by the ring distribution of the water ions. Model computations of the ion distribution function confirm the idea that this function is non-Maxwellian .[7] Moreover, the so-called "ring distribution" was measured directly, and one may believe that the electrostatic broadband noise observed in the wake of the shuttle can be explained theoretically by that mechanism.[8] However, an additional analysis of the electrostatic noise generation mechanism is needed because there are essential differences in plasma parameters between the SAMPIE and PDP experiments-

all the SAMPIE measurements of electrostatic noise (HFT dwells) were performed in ram conditions. The SAMPIE LP used a 5 cm diameter spherical sensor mounted on a fixed boom approximately 100 cm from the surface of the shuttle [9,10], and fluctuations of electric current were measured by using a logarithmic amplifier with the I-V characteristic shown in Fig. 1.[11] Each dwell lasted for 4 ms, and experimental data were represented in digital form: 80 measurements of current at 50 μs intervals.

Spectra of the fluctuations were computed by using the FFT procedure; thus, we are able to study the plasma turbulence within the narrow frequency interval Δf=250-10,000 Hz. According to the purposes of the SAMPIE, the samples of solar cells were placed in the cargo bay of the shuttle, and high negative bias voltages were applied to them to initiate arcing between these cells and the surrounding plasma. It was shown that arcing influences the parameters of the electrostatic noise [2], and we discuss this topic in the last section of the current paper.

Observations

Three examples of HFT dwells with their spectra are shown in Fig. 2-4. The background plasma parameters (electron number density and temperature) were obtained by using the I-V characteristic of the LP.[10] As can be seen, there are no essential differencies among these graphs besides the amplitudes of the fluctuations: the amplitude of the current reaches $i_{max} \approx 0.1\,\mu A$ for the dwell shown in Fig. 2, and the amplitudes are substantially higher for dwells shown in Fig. 3 and Fig. 4 ($i_{max} \approx 0.4\,\mu A$). But if we take

into account the difference in electron number densities for these three dwells, we may conclude that the level of fluctuations $\frac{\delta n_e}{n_e}$ is five times higher for the last dwell (Fig.4).

All spectra demonstrate a sharp cutoff for frequencies $f \geq f_{LH}$. This fact could be considered as an argument in favor of the Ion Acoustic Waves hypothesis because such kind of waves can be excited within the frequency range $F_i < f < f_{LH}$ if the electron temperature T_e is much greater than the ion temperature T_i. . An HFT dwell that was recorded one minute before the dwell shown in Fig. 3 demonstrates almost the same signal shape and spectrum but the amplitude of fluctuations is about five times less (Fig. 5).

One minute (60 seconds) is not a natural time scale for IAW because the calculations of the attenuation rate and instability increment for such waves show very short time intervals (τ=3-100 ms) (Fig. 6). The duration of one dwell (τ_D=4 ms) is not long enough to observe any regular trend in amplitudes although one could believe that the decrease of the amplitude for a time interval t>2 ms is caused by real attenuation (Fig. 3 and Fig. 4). Some measurements were done in a plasma with a relatively low electron number density (Fig. 7). Here, the pressure of neutral gas is about 20% less than for the dwells shown above but, surprisingly, the level of fluctuations is almost one order in magnitude higher. There are no essential differences in spectra between this dwell and other dwells .

For very low electron number density and low pressure of the neutral gas only the instrument noise was registered (Fig. 8). The origin and the characteristics of the observed electrostatic fluctuations must be explained by theory. We interpret these fluctuations in

terms of Ion Acoustic Waves travelling in a weakly ionized plasma layer surrounding the Shuttle.

Interpretation

The Shuttle is surrounded by a gas cloud caused by many different processes accompanying spacecraft operations: outgassing of surfaces, leakage from valves, thrusters firing, etc. [7] Molecules of the gas are moving at the thermal speed in the rest frame of the Shuttle, and ionospheric ions and neutral atoms can be considered an inflow with an average speed V_S=7.8 km/s. If we suggest that the cloud is formed mainly from water vapor with an initial temperature $T_g \le 300\,K$, we may determine the number density of water molecules from measurements of the gas pressure near the Shuttle:

$$n(H_2O) = \frac{p}{k_B T} = 6.4 \cdot 10^{10} \left(\frac{p}{2\,\mu Torr}\right) \cdot \left(\frac{T}{300K}\right)^{-1} cm^{-3} \qquad (1)$$

This value of the number density is a few times more than the number density of the ambient atmospheric gas at flight altitudes (220-310 km). According to direct computations, the water vapor densities at distances about 50 m from the Shuttle can be as large as $n(H_2O) = 2 \cdot 10^9\ cm^{-3}$, and this value reaches $4 \cdot 10^{10}\ cm^{-3}$ in close to the spacecraft surface .[7] It should be noted that water molecules outgassed from the shuttle were directly observed during the flight of STS-39. According to IR emission data the column density of water molecules was equal to $5 \cdot 10^{16} - 3 \cdot 10^{17}\ m^{-2}$ [12,13] , and

these measurements allow us to calculate the number density $n(H_2O) = 2 \cdot 10^{10} - 10^{11}\, cm^{-3}$. Now, we can estimate the mean free path for a water molecule. The thermal speed is equal to

$$V_T = \left(\frac{2k_B T}{m(H_2O)}\right)^{1/2} = 5.3 \cdot 10^4 \left(\frac{T}{300K}\right)^{1/2} \quad \frac{cm}{s} \qquad (2)$$

If we adopt as the cross section for molecular collisions $\sigma = 2 \cdot 10^{-15}\, cm^2$ [14] and the number density of the neutral gas $n_g \approx 10^{10} cm^{-3}$, we will get a rough estimation for the mean free path,

$$l = \frac{1}{\sigma \cdot n_g} = 5 \cdot 10^4\, cm = 0.5\, km \quad , \qquad (3)$$

that is much greater than the linear dimension of the spacecraft (L~10 m). The time interval between two collisions is equal to

$$\tau = \frac{l}{V_T} = 1 \cdot \left(\frac{T}{300K}\right)^{-1/2} s \qquad (4)$$

These estimates allow us to write the radial dependence of the water molecule number density in the simple form [7]:

$$n(H_2O) = n_0 \cdot \left(\frac{L}{L+R}\right)^2 \cdot \exp\left(-\frac{R-L}{l}\right) \qquad (5)$$

Measurements of the electron temperature in the vicinity of the Shuttle are in the range T_e=(0.1-0.3) eV .[10] For IAW, the phase velocity is equal to

$$W_s = \left(\frac{k_B T_e}{m_i}\right)^{1/2} = 7.3 \cdot 10^4 \cdot \left(\frac{T_e}{0.1eV}\right)^{1/2} \frac{cm}{s} \qquad (6)$$

According to the dispersion relation for IAW, the wave length can be calculated as

$$\lambda = \frac{W_s}{f} = 73 \cdot \left(\frac{f}{1kHz}\right)^{-1} \left(\frac{T_e}{0.1eV}\right)^{1/2} \quad cm \qquad (7)$$

where f is a frequency of fluctuations measured in the rest frame of the plasma.

Thus, within the framework of the IAW hypothesis the wave length of fluctuations is less than 3 m for the whole range of the observed frequencies. This means that we may consider the gas layer surrounding the Shuttle as slightly non-homogeneous because of the following inequalities:

$$S_{LP} \leq \lambda_{max} << L << l \qquad (8)$$

In the relations (8) S_{LP} is the distance of the LP from the spacecraft surface.

Neutral water molecules that are ejected from the Shuttle surfaces will be ionized by an electrical charge exchange with ions O^+ having the flow velocity V_0=- 7.8 km/s and temperature $T_+ \leq$1000 K:

$$O^+ + H_2O \rightarrow H_2O^+ + O \qquad (9)$$

Three more reactions should be added to the reaction (9) to write the complete chain of reactions:

$$H_2O^+ + H_2O \rightarrow H_3O^+ + OH \quad (a)$$
$$H_2O^+ + e^- \rightarrow H_2O^* \rightarrow H + OH \quad (b) \qquad (10)$$
$$H_3O^+ + e^- \rightarrow H + H_2O \, and \quad OH + 2H \quad (c)$$

The kinetic equations for the reactions (9) and (10) were solved by using reaction rates tabulated in the work of Paterson and Frank [7]. For particular case

$$n(O^+) = 2 \cdot 10^5 \, cm^{-3} \quad ,$$

$$n(H_2O) = 6 \cdot 10^{10} \, cm^{-3} \quad , and \quad n_e = n(O^+) + n(H_2O^+) + n(H_3O^+)$$

we obtain the ratio

$$x = \frac{n(H_2O^+)}{n(H_2O)} = 3.9 \cdot 10^{-6} \qquad (11)$$

As a result, the plasma comoving the Shuttle can be characterized by an ion number density as large as $(2-3) \cdot 10^5 \, cm^{-3}$. In the rest frame of the shuttle these ions are under the influence of a magnetic field $\boldsymbol{B}$ and an induced electric field $\boldsymbol{E}$ that is perpendicular to both vectors V_s and $\boldsymbol{B}$, and the electric field strength is equal to

$$E = V_s \cdot B \cdot \sin\Theta = 0.23 \cdot \left(\frac{B}{0.3Gs}\right) \cdot \sin\Theta \quad \frac{V}{m} \qquad (12)$$

where Θ is the angle between the Earth magnetic field and the velocity of the spacecraft (Fig. 9).

It is well known that electrically charged particles will drift with speed $V_D = V_s \cdot \sin\Theta$ in a direction that is perpendicular to both electric and magnetic fields. The angle between

the Shuttle velocity and the magnetic field varied from Θ=-65° to Θ=90° during the experiments that are considered in the current paper. This means that the projection of drift velocity directed to the surface of the shuttle $V_{\perp}$ was always greater than the projection along the surface $V_{||}$:

$$\frac{V_{\perp}}{V_{//}} = |\tan\Theta| > 1 \qquad (13)$$

We can conclude that there were two streams of ions with relative velocity

$$V_r = -V_s - V_D \ . \qquad (14)$$

Thus, it is possible to use the dispersion equation for IAW that may be written in the following form [15]:

$$1 + \frac{1}{k^2\Lambda_1^2} + \frac{1}{k^2\Lambda_2^2} - \left(\frac{\omega_1}{\omega}\right)^2 - \frac{\omega_2^2}{\left(\omega - k\cdot V_r\cdot\cos\alpha\right)^2} = 0 \qquad (15)$$

where $\Lambda^2 = \dfrac{k_B T_e}{4\pi\cdot e^2 n_e}$ is the Debye length, $\omega_{1,2}$ are the ion plasma frequencies for oxygen and water ions respectively, and α is the angle between the wave vector $\boldsymbol{k}$ and the relative velocity V_r.

The fourth order equation (15) has complex roots (instability) if the following inequality can be fulfilled:

$$V_r^2\cos^2\alpha < W_s^2\cdot\frac{\left(\omega_1^{1/3}+\omega_2^{1/3}\right)^3}{\omega_1+\omega_2} \qquad (16)$$

To obtain the inequality (16) we suggest $T_{e1} = T_{e2}$, and we take into account that the masses of oxygen and water ions are almost equal to each other.

For the simplest example $\omega_1 = \omega_2$, the condition of instability (16) can be written in the form

$$|\cos\alpha| < 2 \cdot \frac{W_s}{V}, \qquad (17)$$

where $V = V_s \cos\Theta$.

It is seen from the expression (17) that the cone of instability is wide for $\Theta \approx 90°$. But the dispersion relation does not have complex roots when $\Theta = \pi/2$. In that case, the drift velocity is equal to the Space Shuttle speed exactly, and there is no any relative motion of the two kinds of ions; thus, the two-stream instability does not work when the spacecraft velocity is perpendicular to the Earth magnetic field.

Now we can consider some specific experiments. For example, the angle between vectors V_s and B is equal to $\Theta = -66.4°$ (Fig.2). It is easy to calculate the IAW phase speed $W_s = 8 \cdot 10^4$ cm/s and $|\cos\alpha| < 0.5$. The complex frequency (the growing mode only) can be determined from the Eq.(15):

$$\begin{aligned} \frac{\omega}{kW_s} &= 0.5 + i \cdot 0.34 \quad (\cos\alpha = 0.25) \\ \frac{\omega}{kW_s} &= 0.9 + i \cdot 0.24 \quad (\cos\alpha = 0.45) \end{aligned} \qquad (18)$$

For different ion number densities $\frac{\omega_1}{\omega_2} = 2$ we obtain almost the same result:

$$\frac{\omega}{kW_s} = 0.6 + i \cdot 0.33 \quad (\cos\alpha = 0.25) \qquad (19)$$

During experiment E_62-2/03 the electron temperature was substantially higher (Fig. 3). The IAW speed was equal to $W_s = 9.5 \cdot 10^4$ cm/s, and the relative velocity of the ion streams

was equal to $V=1.36\cdot10^5$ cm/s. It is seen that for this particular experiment the "beam" velocity is almost equal (a little higher) to the IAW phase velocity. Such a condition is optimal for energy transfer from flux kinetic energy to fluctuations, and the rate of instability is high for all the magnitudes of angle between wave vector and stream velocity (see Eq. (17)). This result depends on the relation between ion number densities only weakly:

$$\frac{\omega}{kW_s} = 0.5 + i\cdot 0.34 \quad (\cos\alpha = 0.5, \quad \omega_1 = \omega_2)$$
$$\frac{\omega}{kW_s} = 0.78 + i\cdot 0.25 \quad (\cos\alpha = 0.5, \quad \omega_1 = 0.1\omega_2) \qquad (20)$$
$$\frac{\omega}{kW_s} = 0.22 + i\cdot 0.25 \quad (\cos\alpha = 0.5, \quad \omega_1 = 10\omega_2)$$

When the angle between the spacecraft velocity and the magnetic field is almost equal to 90° the relative speed is less than the IAW phase speed, and the conditions for the two-stream instability are broken in this case. The dispersion relation (15) has two real roots for any values ω_1 and ω_2:

$$\frac{\omega}{kW_s} = \pm 1 \qquad (21)$$

Due to the IAW attenuation, we should not observe the electrostatic noise during the time interval $t\approx 5$ min which is needed to change the angle Θ from 85 to 95 degrees (Fig. 10). However, fluctuations were observed even during the dwell recorded for $V_s \perp B$ (Fig. 4). Such a situation was discussed by Pickett et al.[6], and they suggested that a modified two-stream instability (MTSI) could explain the observational data obtained in their experiment for the wake of the shuttle. MTSI generates fluctuations with

frequencies near the lower hybrid resonance frequency (few kHz), and some nonlinear processes should be considered to explain the observed spectrum that has significant amplitudes at frequencies as low as a few Hz.

If we confront our LP data obtained for B_x=0 (Fig.4) with data obtained for $B_x \leq |B|$ (Fig. 3 and Fig. 5), we may suggest that the nature of the turbulence is the same in all three cases because the shape of signals and their spectra are essentially identical. One of the possibilities to explain the IAW instability is the gradient instability caused by electron and ion number density gradients with a scale $a = \left(\frac{1}{n_i} \cdot \frac{dn_i}{dR}\right)^{-1} \approx 5m$ (see Eq. (5)).

The dispersion relation can be written in the following form [16]:

$$\frac{1}{\Lambda_e^2} + k^2 - \frac{\omega_i^2}{\omega^2} \cdot k^2 \cdot \left(1 + \frac{1}{i \cdot k \cdot n_i} \cdot \frac{dn_i}{dR} \cdot \sin\varphi\right) = 0 \qquad (22)$$

where φ is the angle between the wave vector **k** and the Earth magnetic field **B**.

Taking into account that the Debye length is much smaller than the wave length, we can represent the increment of instability in the following form:

$$\frac{\gamma}{\omega} = \frac{1}{2} \cdot \left| \frac{1}{k \cdot n_i} \cdot \frac{dn_i}{dR} \right| \qquad (23)$$

where ω obeys the Eq. (21).

It should be noted that the Eq.(23) is valid when the angle between the wave vector $\boldsymbol{k}$ and the magnetic field $\boldsymbol{B}$ is not close to zero, but $\frac{k_y}{k_z} < 1, and \quad \frac{k_x}{k_z} < 1$ (k_y is the projection of the wave vector on the direction that is perpendicular to both vectors $\boldsymbol{B}$ and **grad** n_i.). The ratio (23) can be easily estimated for the considered frequency range: γ/ω= 0.005-0.1. The attenuation rate of IAW depends on the ratio of the electron temperature to the ion temperature [17] (Fig. 11). The electron temperature is measured for each dwell, and we can use these data for further calculations.

We can estimate the ion temperature by hypothesizing that the main ion component of the plasma is water ions generated by a charge exchange process. Thus, we can assume that T_i <300 K. Moreover, the IAW attenuation rate depends on the angle between the wave vector and the magnetic field [18] (Fig. 6). If we compare the attenuation rates mentioned above with increment (23), we see that there is enough room for an instability of IAW even in ram conditions with $V_s \perp B$ if $\frac{T_e}{T_i} \geq 10$.

The Influence of Arcing

As was mentioned above, HFT data were also obtained during the experiments when arcs occurred. First of all, there is a significant difference in amplitudes between signals with arcing and without them (Fig. 12). For this one particular dwell, the amplitude of current fluctuations is as large as 2 μA. The number of arcs, the maximum current for each arc, and the duration of the arc were measured by a special counter. One example of

data obtained during experiment E_60-1/01 is shown in Fig. 13. There is a strong correlation between the number of arcs observed in an experiment and the amplitude of fluctuations (Fig. 14). All these facts show that there is an influence of arcs on the HFT data. We believe that the large amplitude of LP current is caused by rapid changes in the spacecraft potential due to arcing. When arcing occurs, the difference of potentials between the shuttle and the surrounding plasma changes $\Delta V \approx 2-3$ V for the moment of each arc. Because the duration of each arc is equal to 0.1-0.5 μs, the measured value of LP current can be estimated as

$$\Delta I_{\max} = \frac{N_{arc}}{\tau_{exp}} \cdot \tau_{dwell} \cdot \left(\frac{\partial I_{sat}}{\partial V} \cdot \Delta V \right) \qquad (24)$$

For example, during one experiment, N_{arc}=1500, the duration of the experiment τ_{exp}=60 s, and τ_{dwell}=4 ms. The value of the expression in the parenthesis can be obtained from appropriate sweep data (one example is shown in Fig. 15). The result of the calculation, $\Delta I_{max} \approx 2$ μA, is in agreement with the measurements.

According to theoretical considerations, the spectrum of fluctuations in the plasma should have the following form: [18]

$$D(f) = \frac{A}{f} \cdot F\left(\frac{f}{f_e} \right) \qquad (7)$$

where A=Const, and $F(f)$ is a slow function of frequency. In reality, we obtained $D(f) \propto f^{-0.76 \pm 0.2}$ for the average spectrum without arcing, in agreement with expectations (Fig. 16).

We see from the present work that fluctuations with a broad spectrum are developed in the plasma surrounding the shuttle.

Conclusions

During the Solar Array Module Plasma Interactions Experiment (SAMPIE) fluctuations in the electron number density were observed in ram conditions. The amplitudes of these fluctuations were as large as 10^{-3} - 10^{-4} from the background density at frequencies f= 250-6500 Hz. The measurements of the Earth magnetic field allow us to show that this frequency range is inside the interval $F_i < f < f_{LH}$; thus, we suggest that Ion Acoustic Waves were observed. An additional argument in favor of the hypothesis of IAW is the inequality between ion and electron temperatures. Measurements have determined that the electron temperature varied from $0.1 \leq T_e \leq 0.3$ eV.[10] According to Patterson and Frank[7] the ion temperature should be substantially lower : $T_i < 0.03$ eV. This value of ion temperature agrees with measurements of the pressure of neutral gas around the shuttle (Fig. 17) and our estimations of the number density of water molecules (see also Eq.(1)).

These facts named allow us to adopt the basic model of the gas layer around the shuttle that was elaborated by Paterson and Frank.[7] Two kinds of instabilities were suggested for explanation of the origin of IAW: the two-stream instability that works when the angle between the spacecraft velocity and the magnetic field is not too close to a right angle, and the gradient instability that works for situations when the magnetic field and velocity of the shuttle are perpendicular to each other. It should be noted that the last instability is weaker than the first one, and we could observe the transition between the two regimes if the dwell would last for several minutes at least. More measurements need to be done,

particularly for the frequency range 20-100,000 Hz, to allow an understanding of the nature of the observed turbulence.

Acknowledgments

We thank Dr. W. Mackey for useful remarks.

This work was performed while B.V. Vayner held a National Research Council-NASA/LeRC Research Associateship.

References

[1]*Ferguson, D.C. et al.*, Preliminary Results From the Flight of the Solar Array Module Plasma Interactions Experiment (SAMPIE), NASA/LeRC-SEEB, 1994

[2]*Vayner, B.V., and Ferguson, D.C.* Electrostatic Noise in the Plasma Environment Around the Shuttle, 26th AIAA Plasmodynamics and Lasers Conf., June 19-22, 1995, San Diego, CA, Paper AIAA 95-1944

[3]*Siskind, D.E., Raitt, W.J., Banks, P.M., and Williamson, P.R.* Interactions Between the Orbiting Space Shuttle and the Ionosphere, Planet Space Sci., Vol.32, pp.881-896, 1984

[4]*Murphy, G., Pickett, J., D'Angelo, N., and Kurth, W.S.* Measurements of Plasma Parameters in the Vicinity of the Space Shuttle, Planet Space Sci., Vol.34, pp.993-1004, 1986

[5]*Gurnett, D.A., Kurth, W.S., and Steinberg, J.T.* Plasma Wave Turbulence Around the Shuttle: Results From the Spacelab-2 Flight, Geophys. Res. Lett., Vol.15, pp.760-763, 1988.

[6]*Pickett, J.S., D'Angelo, N., and Kurth, W.S.* Plasma Density Fluctuations Observed During Space Shuttle Orbiter Water Releases, Journal of Geophys. Res., Vol.94, pp.12,081-12,086, 1989

[7]*Paterson, W.R., and Frank, L.A.* Hot Ion Plasmas From the Cloud of Neutral Gases Surrounding the Space Shuttle, Journal of Geophys. Res., Vol.94, pp.3721-3727, 1989

[8]*Kurth, W.S., and Frank, L.A.* Spacelab-2 Plasma Diagnostic Package, Journal of Spacecraft and Rockets, Vol.27, pp.70-75, 1983

[9]*Hillard, G.B., and Ferguson, D.C.* Solar Array Module Plasma Interactions Experiment (SAMPIE): Science and Technology Objectives, Journal of Spacecraft and Rockets, Vol.30, pp.488-494, 1993

[10]*Morton, T.L., Ferguson, D.C., and Hillard, G.B.* Ionospheric Plasma Densities and Temperatures Measured by SAMPIE, 33rd Aerospace Meeting, Jan.9-12, 1995, Reno, NW, Paper AIAA 95-0841

[11]*Bozich, R.* Private communication , 1994

[12]*Dean, D.A., Huppi E.R., Smith, D.R., Nadile, R.M. and Zhou, D.K.* Space Shuttle Observations of Collisionaly Excited Outgassed Water Vapor, Geophys. Res. Letters, Vol.21, No7, pp.609-612, 1994

[13]*Zhou, D.K., Pendleton, W.R., Bingham, G.E., Steed, A.J., and Dean, D.A.* Infrared Spectral Measurements (450-2500 cm^{-1}) of Shuttle-Iduced Optical Contamination, Geophys. Res. Letters, Vol.21, No7, pp.613-616, 1994

[14]*Kaplan, S.A., and Pikel'ner, S.B.* Physics of Interstellar Medium, Moscow , Nauka, 1979

[15]*Akhiezer, A.I., Akhiezer, I.A., Polovin, R.V., Sitenko, A.G., and Stepanov, K.N.* Electrodynamics of Plasma, Moscow, Nauka, 1974

[16]*Timofeev, A.V.* Dissipative Instability of a Weakly Ionozed Inhomogeneous Plasma in a Uniform External Nagnetic Field, Soviet Physics-Technical Physics, Vol.8, pp.682-685, 1964

[17]*Krall, N.A., and Trivelpiece, A.W.* Principles of Plasma Physics, McGRAW-Hill Book Co., NY, 1973

[18]*Al'pert, Ya.L.* Space Plasma, Vol.1, Cambridge University Press, Cambridge, MS, 1990

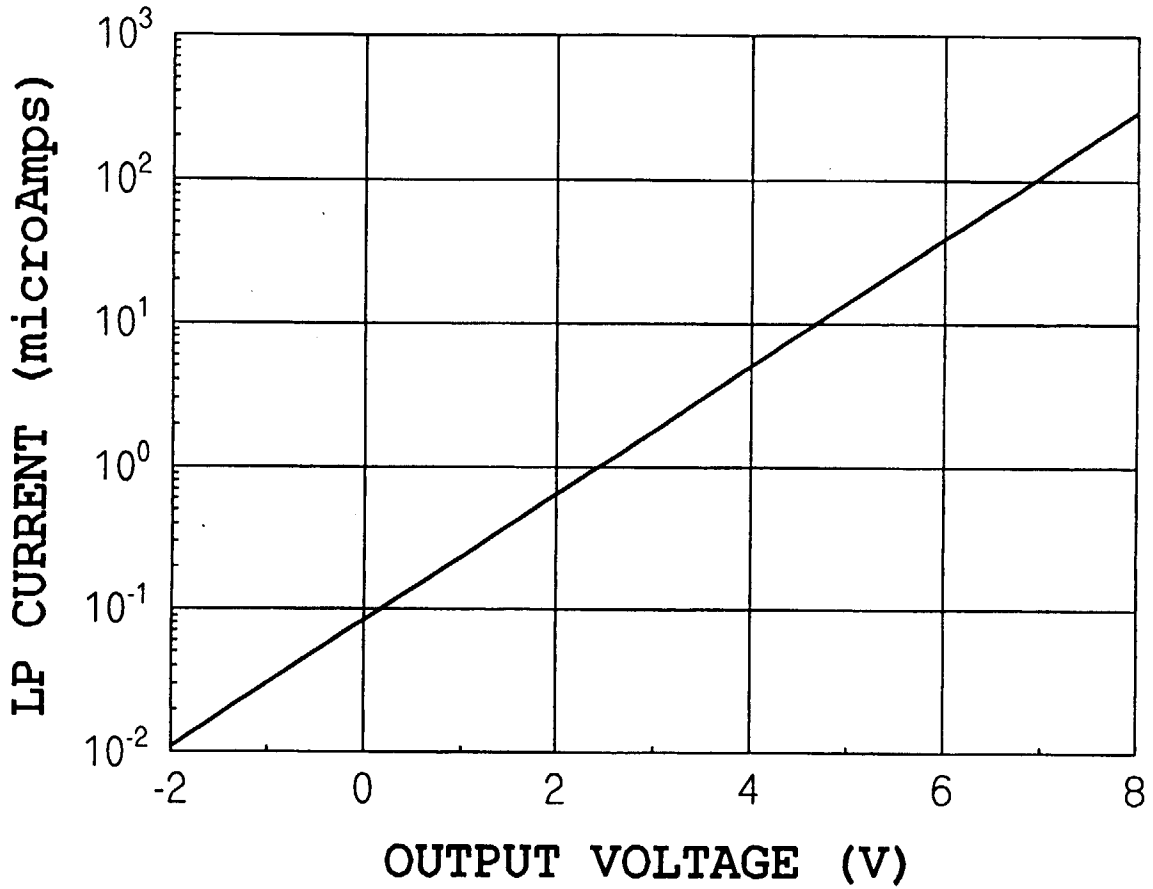

Fig.1 Voltage-current characteristic of the Logarithmic Amplifier

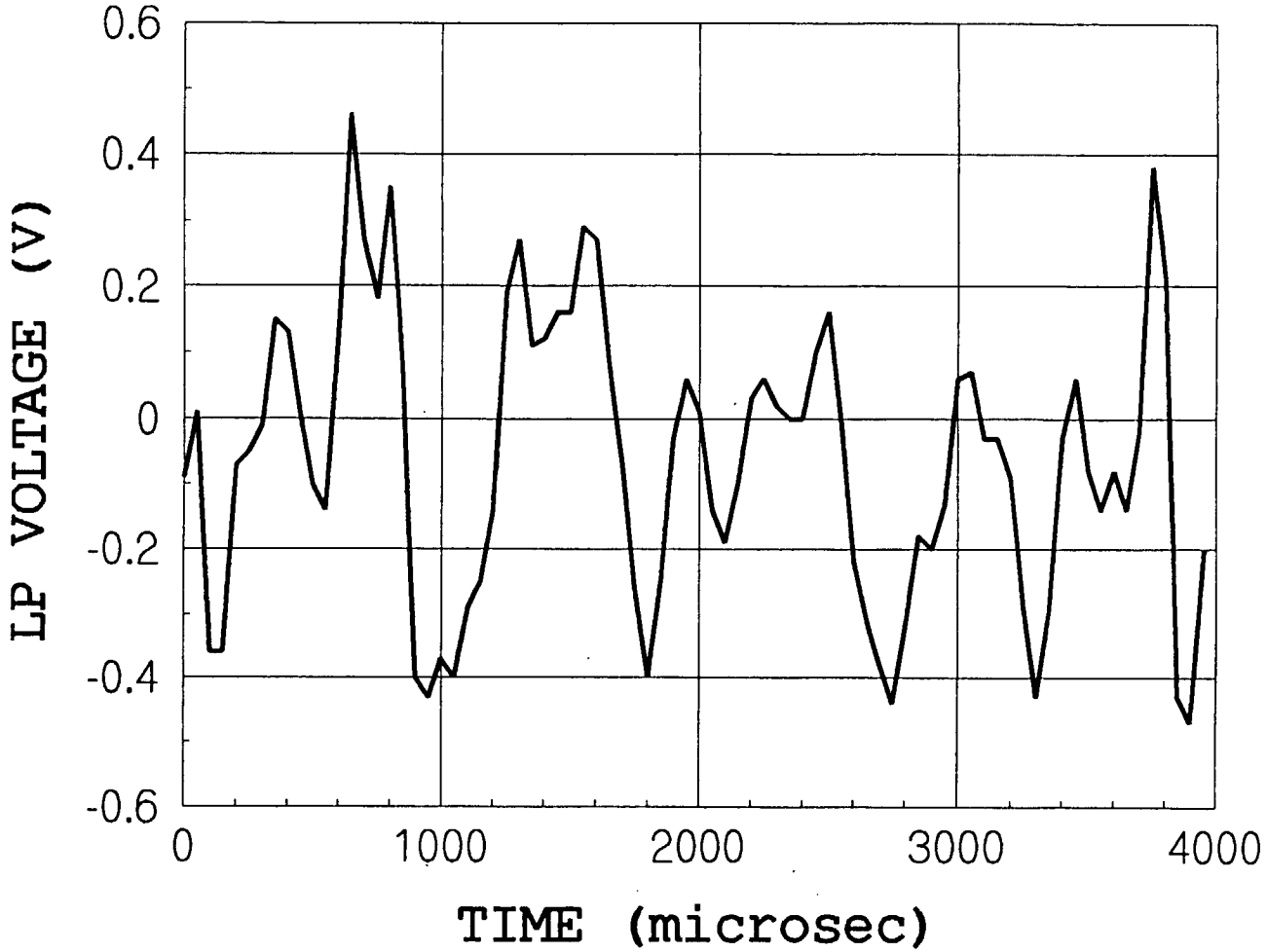

Fig.2a HFT dwell recorded during the experiment E_44-2/01.
MET 7/15:43, electron number density $5.4\times10^{5}cm^{-3}$
electron temperature 0.12eV
and neutral gas pressure 2.27 microTorr.

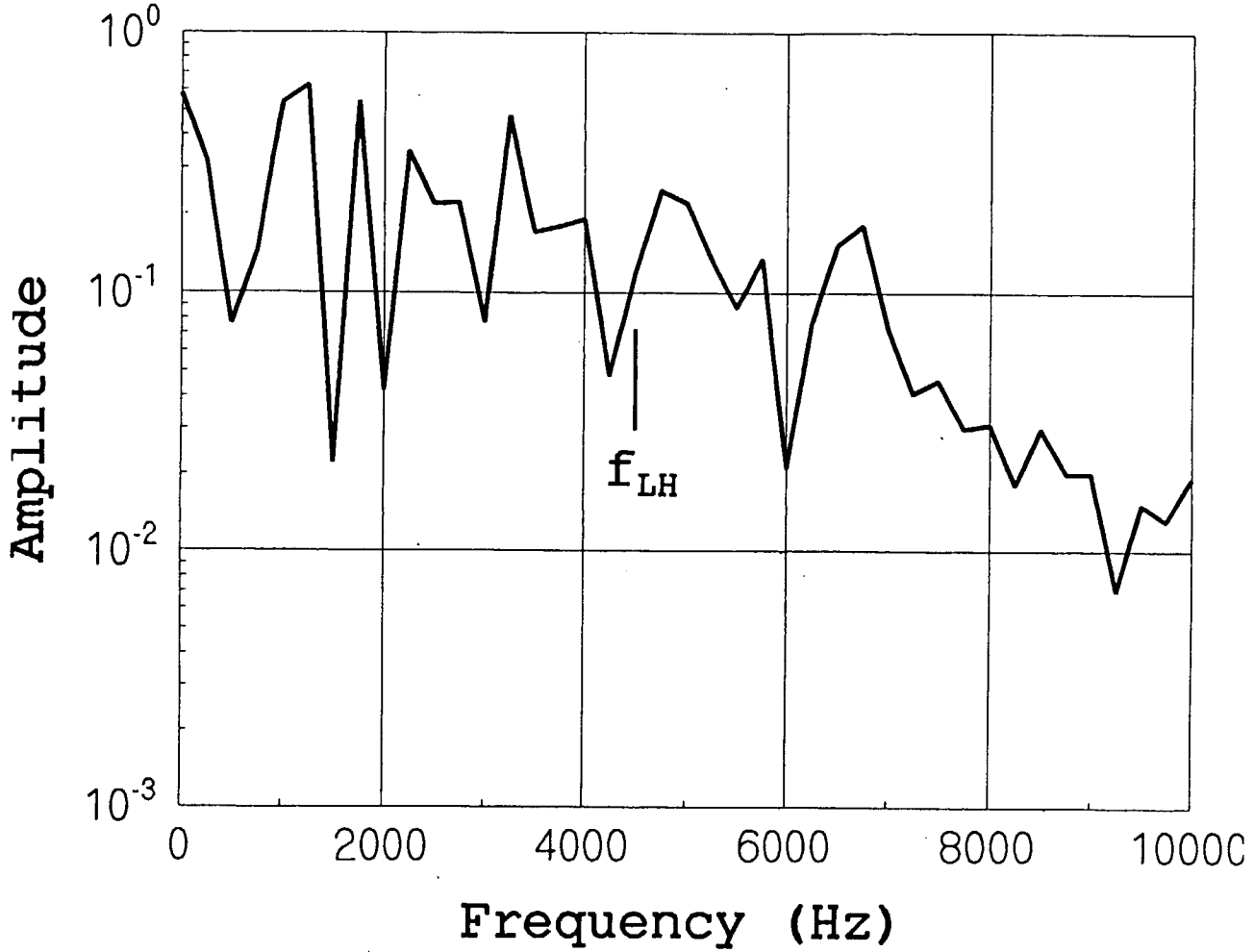

Fig. 2b The spectrum of signal shown above. Magnetic field strength B=0.25 Gs, and angle between B and the velocity of shuttle Θ=-66.4°.

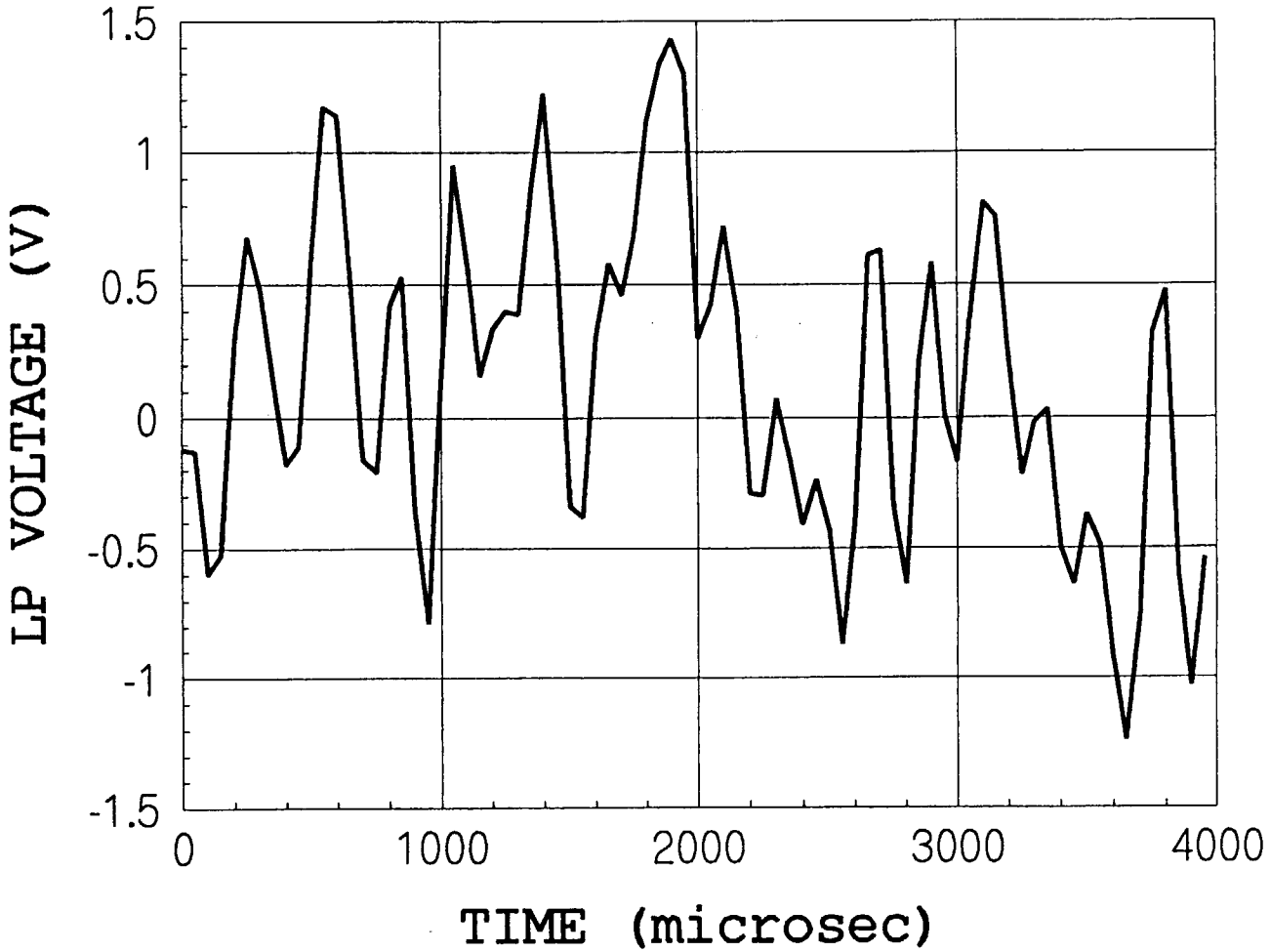

Fig.3a Experiment E_62-2/03. MET 7/23:40, $n_e=4.7\times10^5 cm^{-3}$, $T_e=0.17$ eV, and p=2.1 μTorr

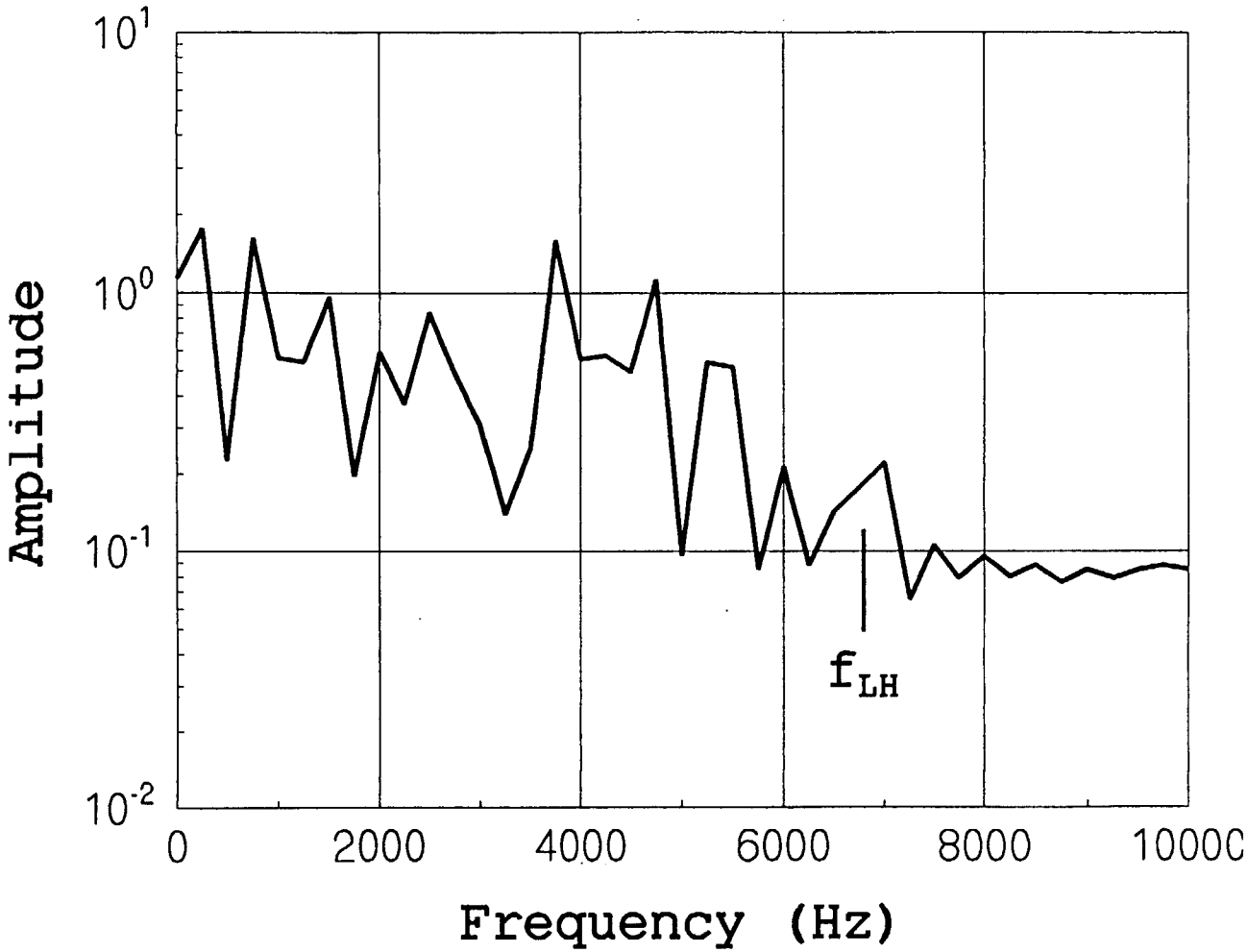

Fig.3b The spectrum of signal shown in Fig. 3a.
B=0.46 Gs, and Θ = -80°

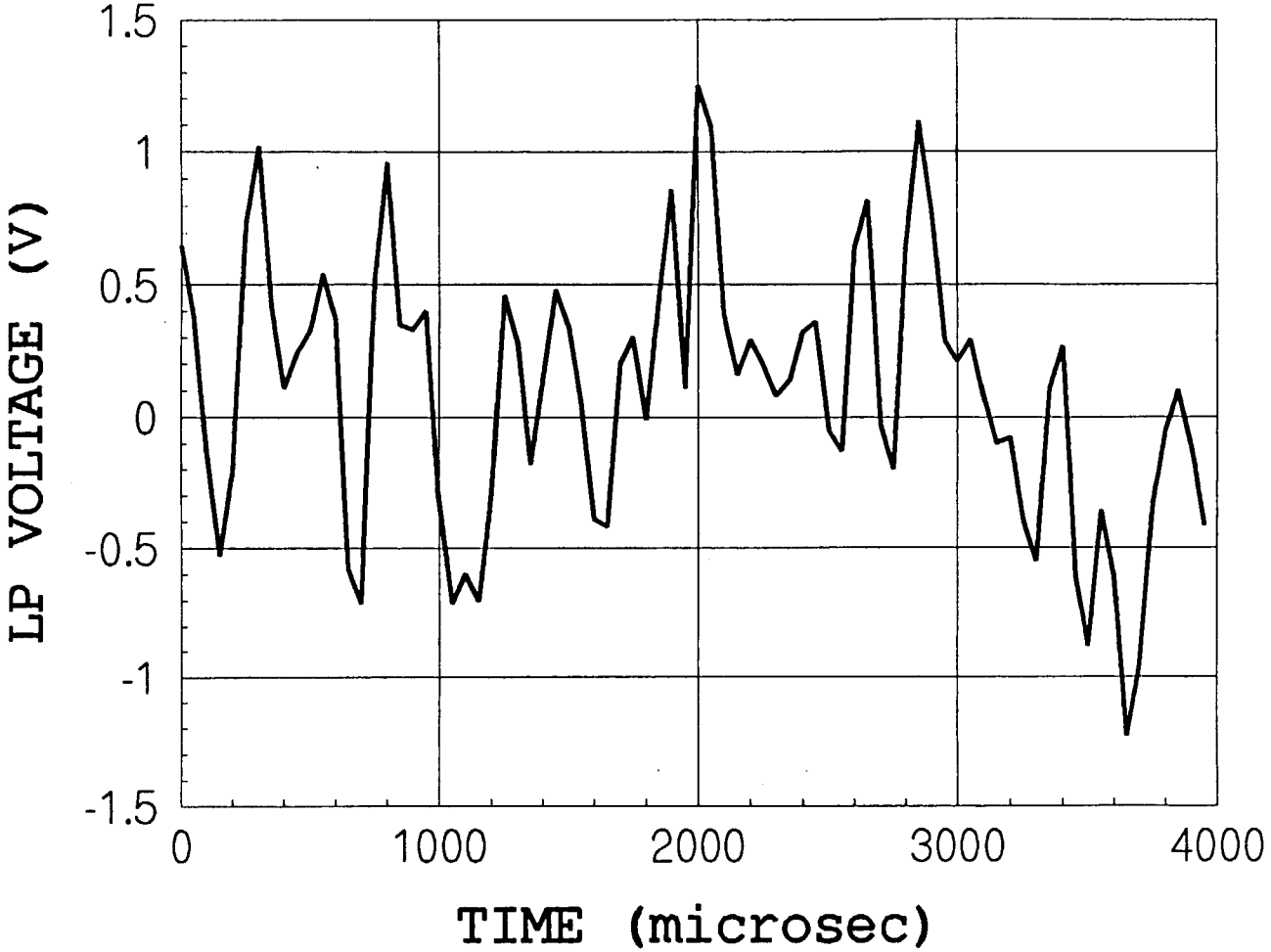

Fig.4a Experiment E_48-2/01. MET 7/22:54, $n_e=6\times10^5 cm^{-3}$, $T_e=0.1$ eV, and p=1.86 μTorr

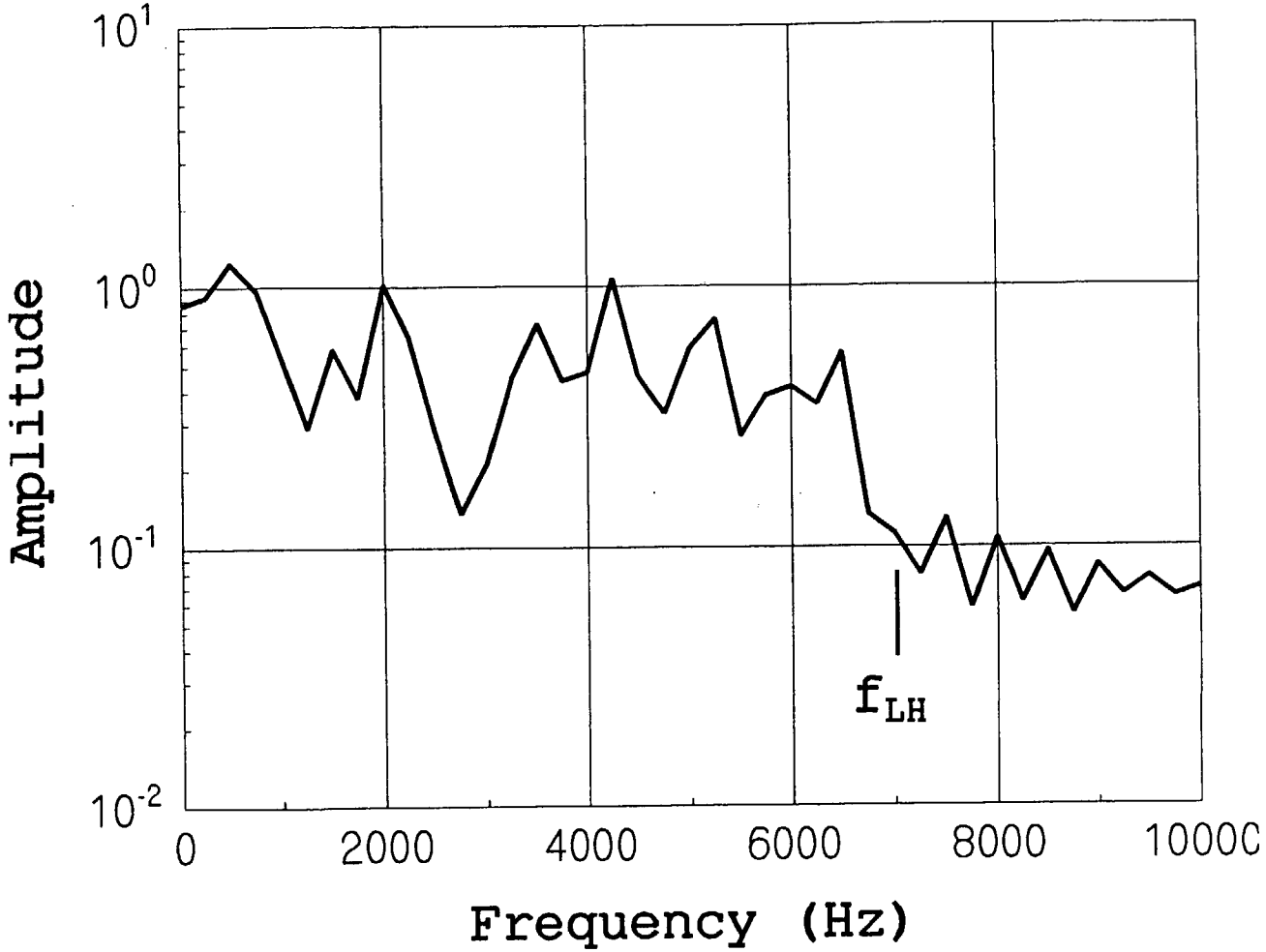

Fig.4b The spectrum of signal shown in Fig. 4a. B=0.52 Gs, and $\Theta = 90^{\circ}$

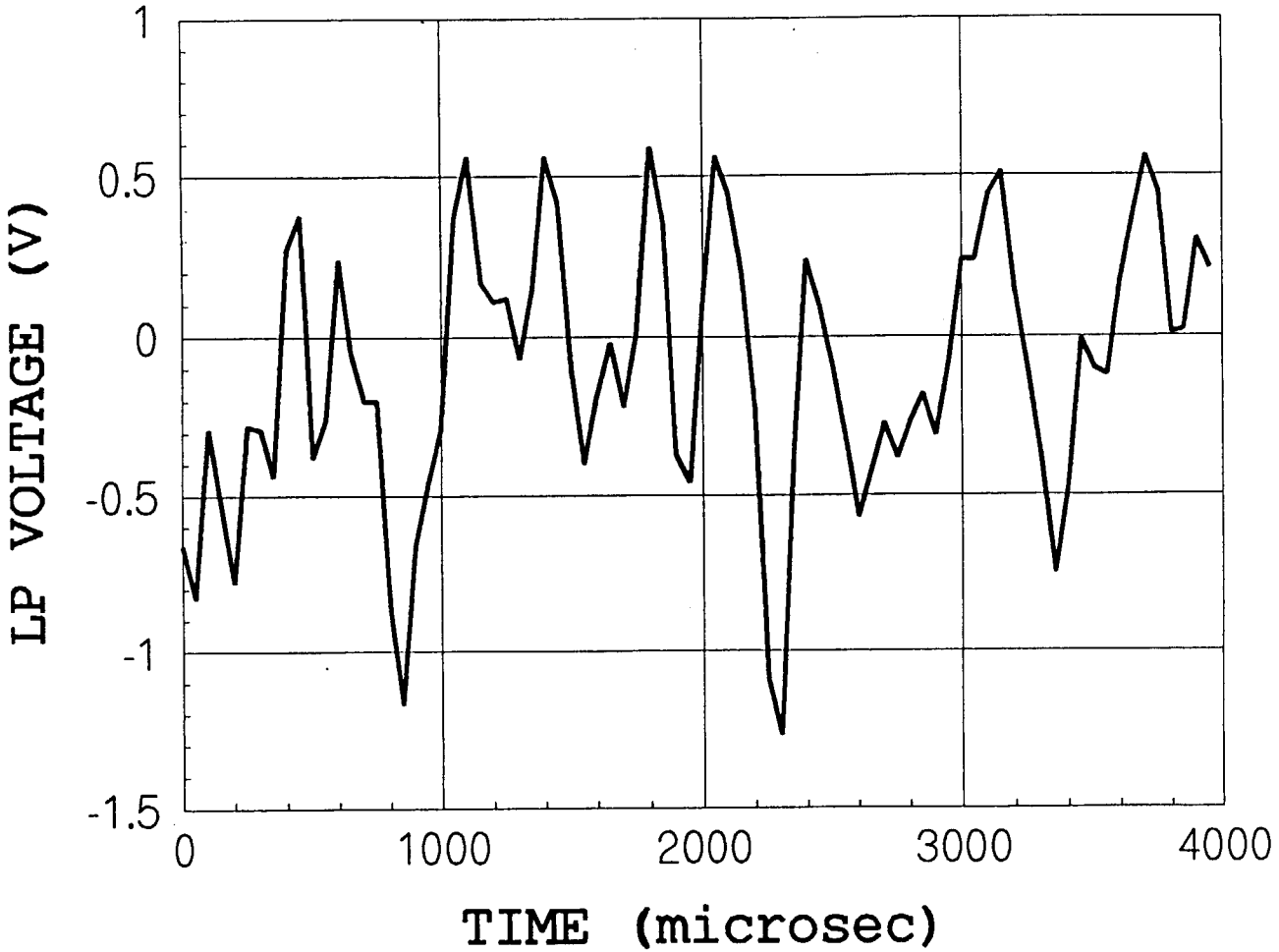

Fig.5a Experiment 62_2/02. MET 7/23:39, n_e=3.8×10^{5}cm^{-3}, T_e=0.17 eV, and p=2.2 μTorr. All parameters are almost the same as in Fig.3, but the amplitude of fluctuations is about five times less.

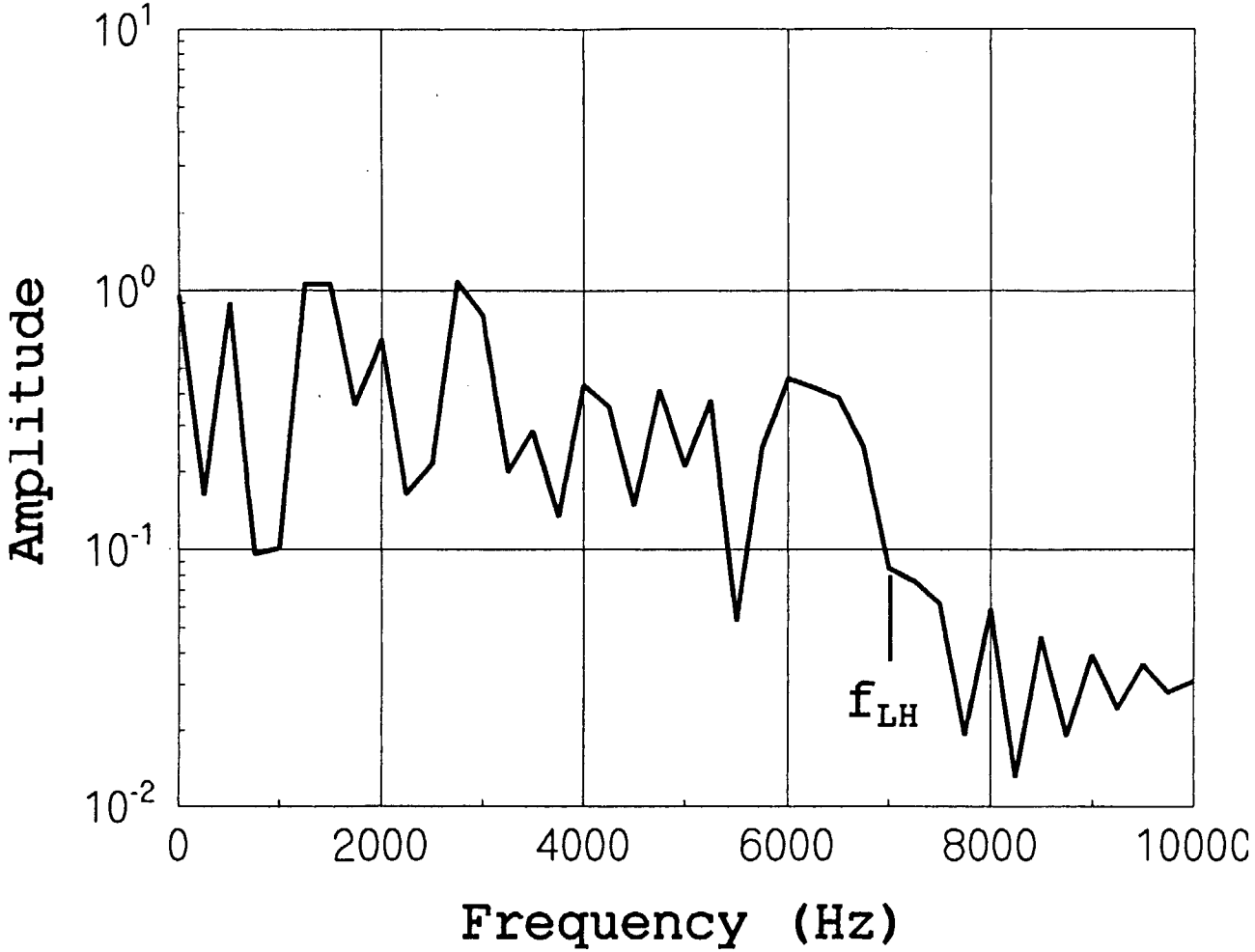

Fig.5b This spectrum demonstrates very sharp decline for frequencies $f \geq f_{LH}$

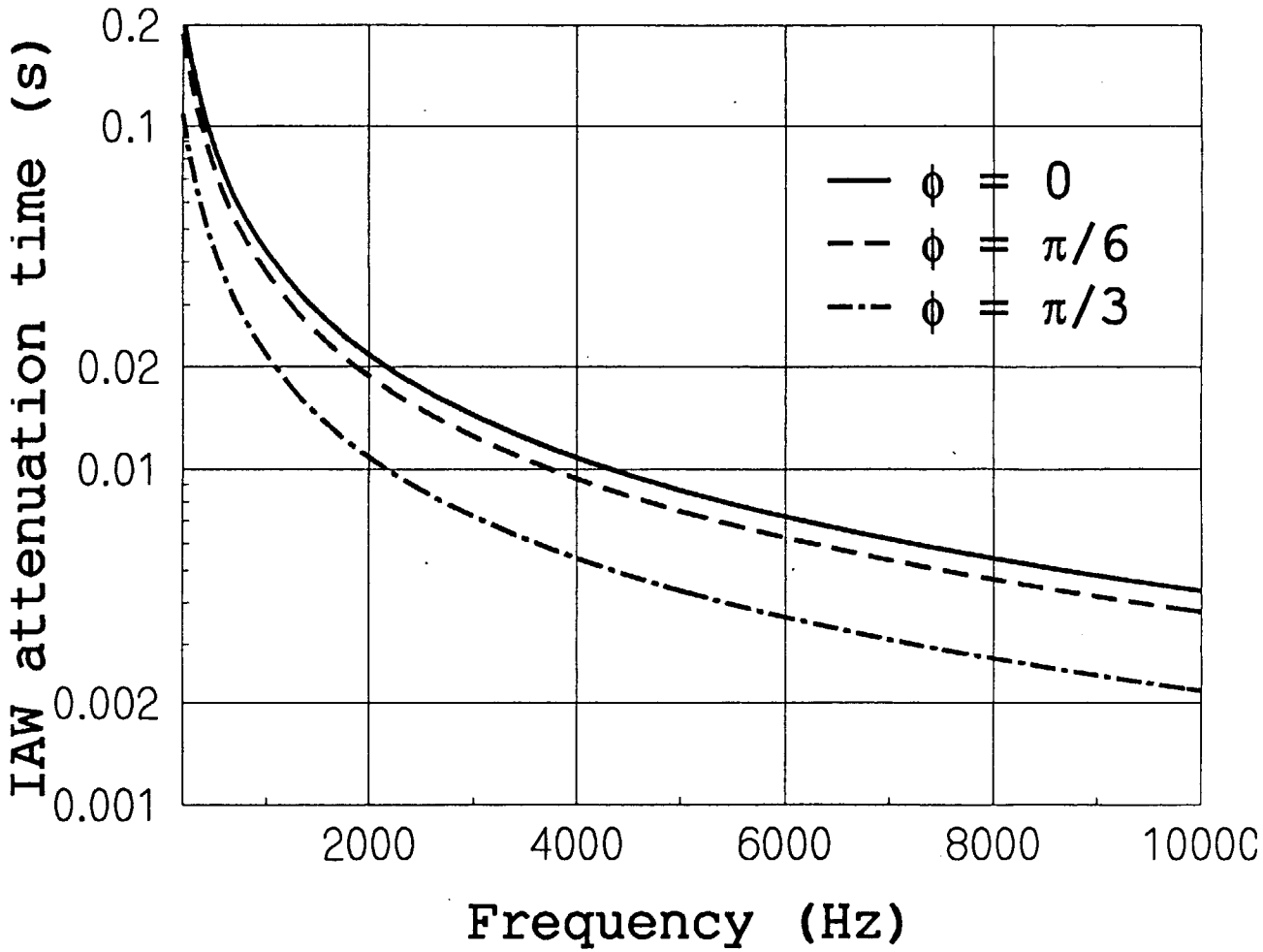

Fig. 6 IAW attenuation time vs. frequency for three magnitudes of angle between the Earth magnetic field and the wave vector (ϕ). (T_e/T_i=15)

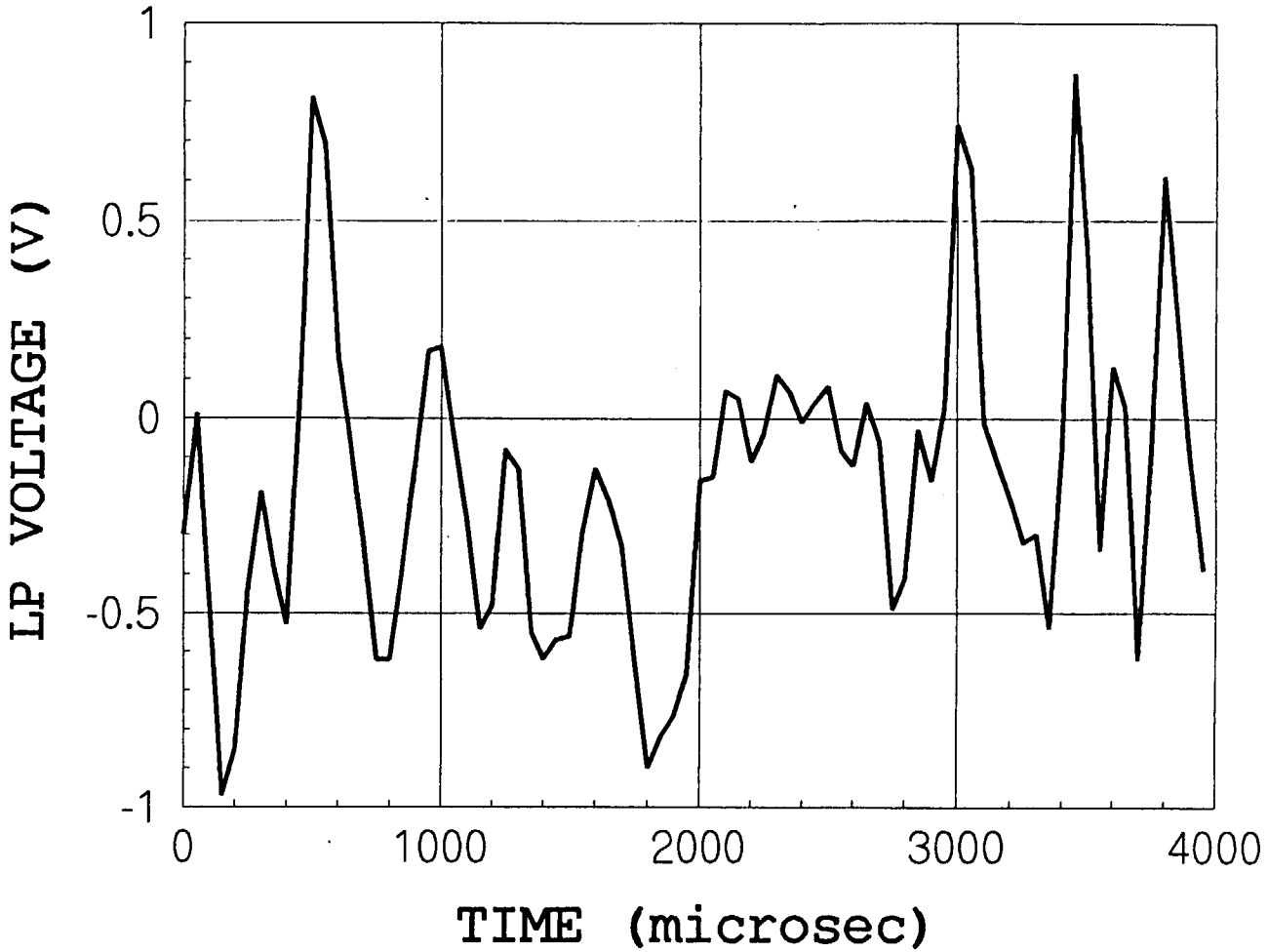

Fig.7a Experiment E_46-1/01, MET 7/15:57, n_e=4.3×10^4 cm^{-3}, T_e=0.14 eV, and p=1.85μTorr

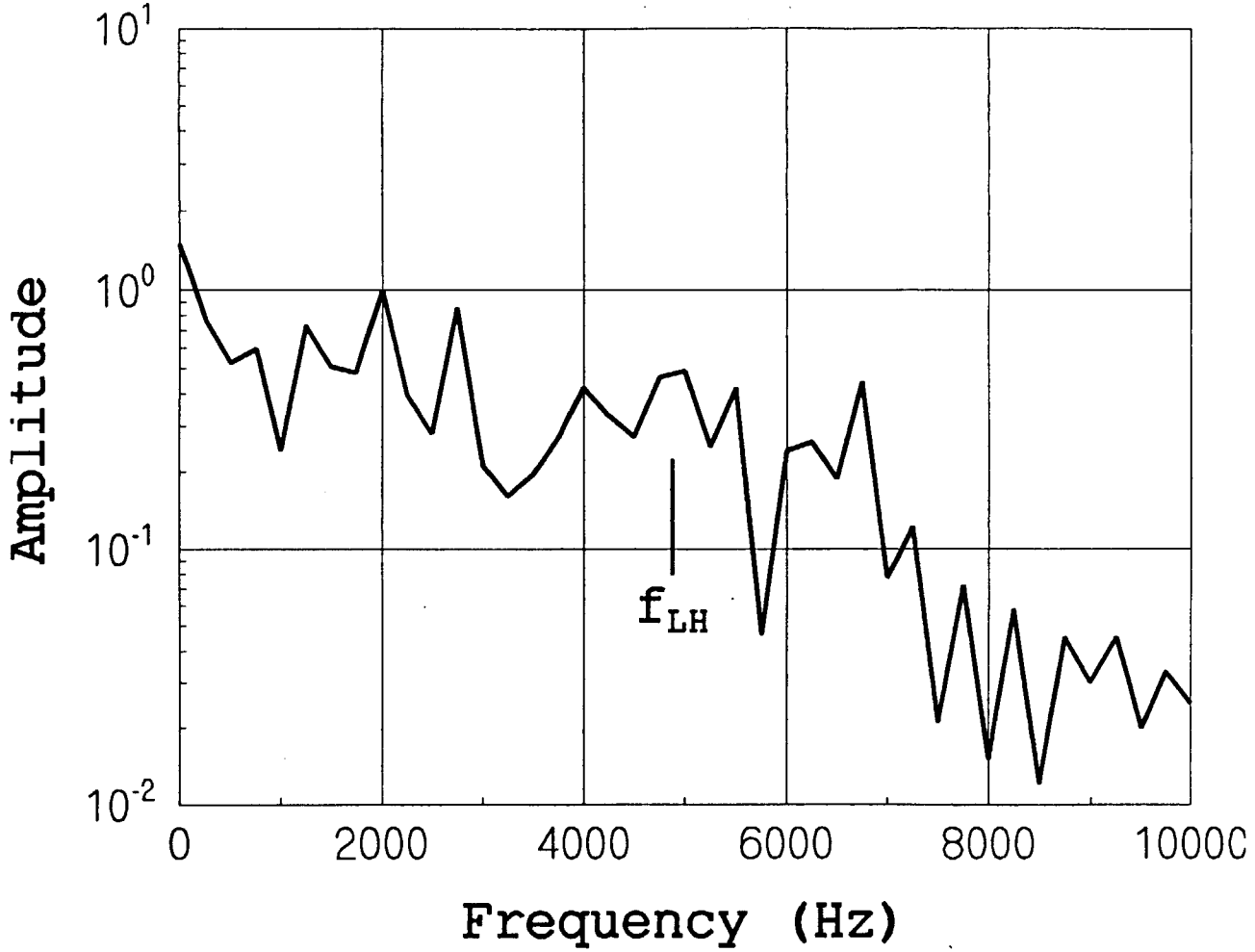

Fig.7b The spectrum of signal shown in Fig. 7a.
B=0.33 Gs, and Θ = 74°

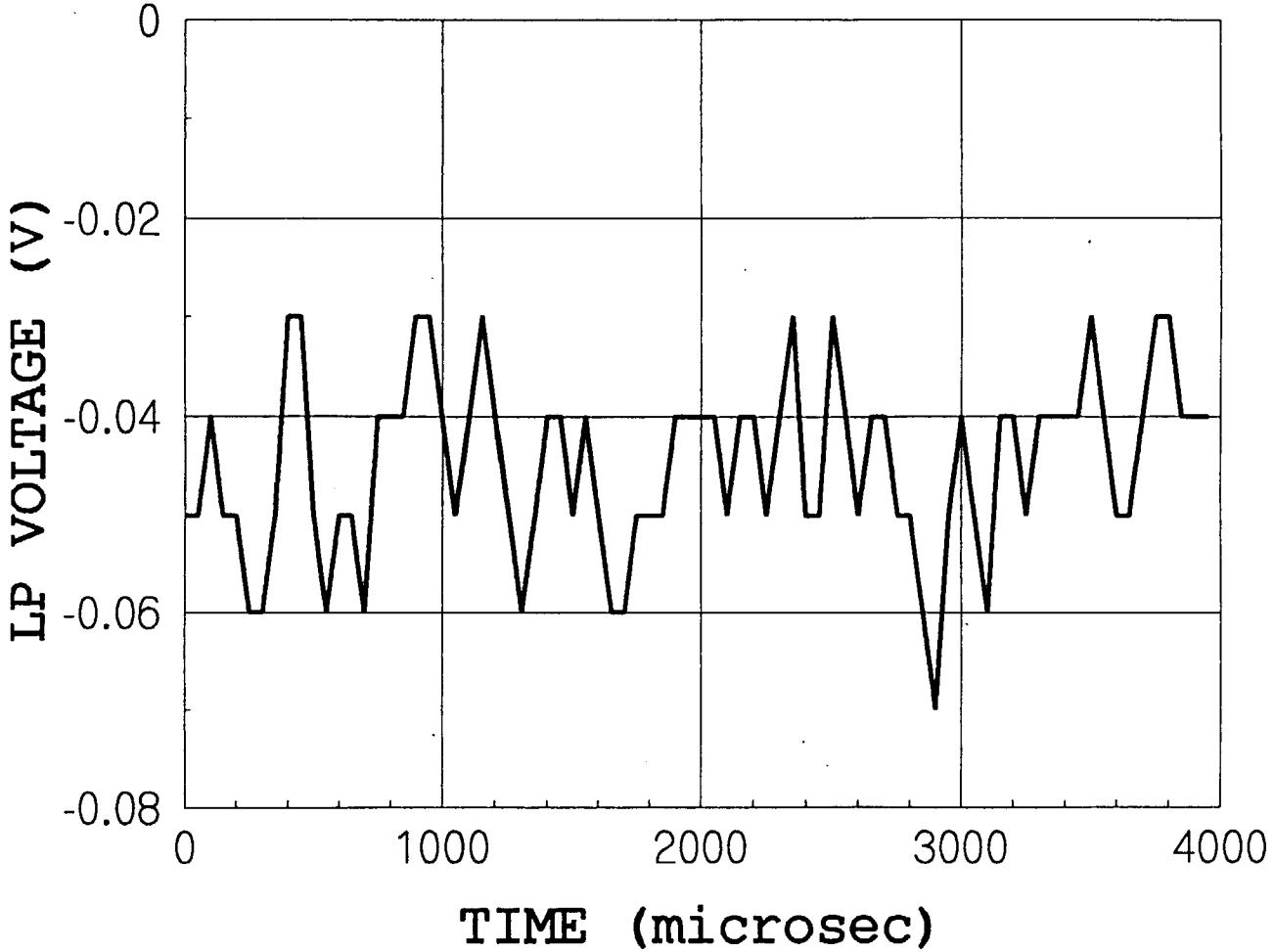

Fig.8 Experiment E_52-12. MET 10/06:27, $n_e=3\times10^4$ cm^{-3}, $T_e=0.1$ eV, and p=0.665μTorr. The instrument noise is registered for low electron number density and low pressure of the neutral gas.

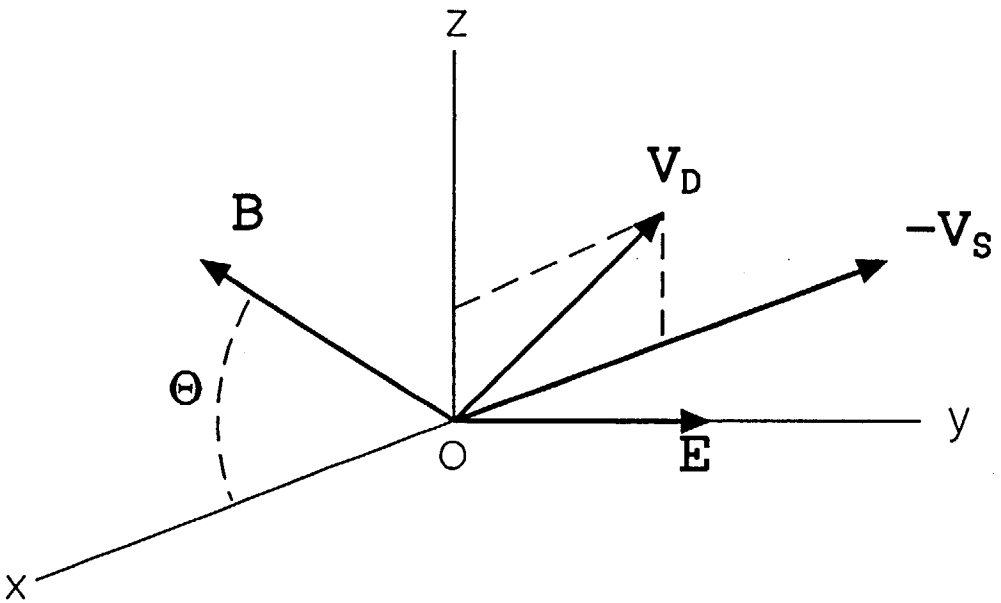

Fig. 9 The spacecraft velocity is directed along x axis. The vector of magnetic field is placed on xOz plane, and the induced elctrical field is perpendicular to both vectors B and V_s. The vector of drift velocity V_D is perpendicular to both vectors B and E.

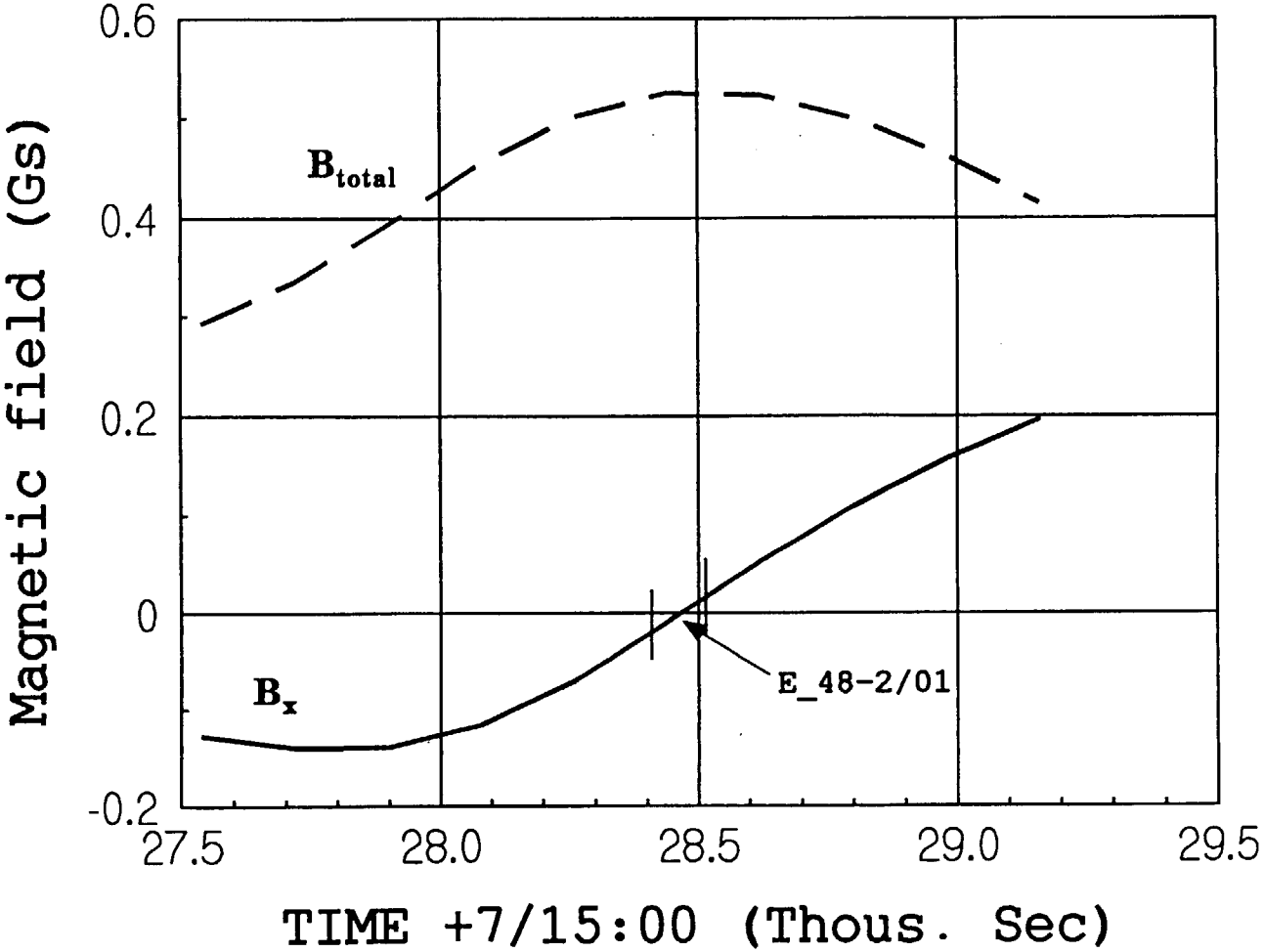

Fig. 10 The magnetic field strength vs. time started at MET 7/15:00.

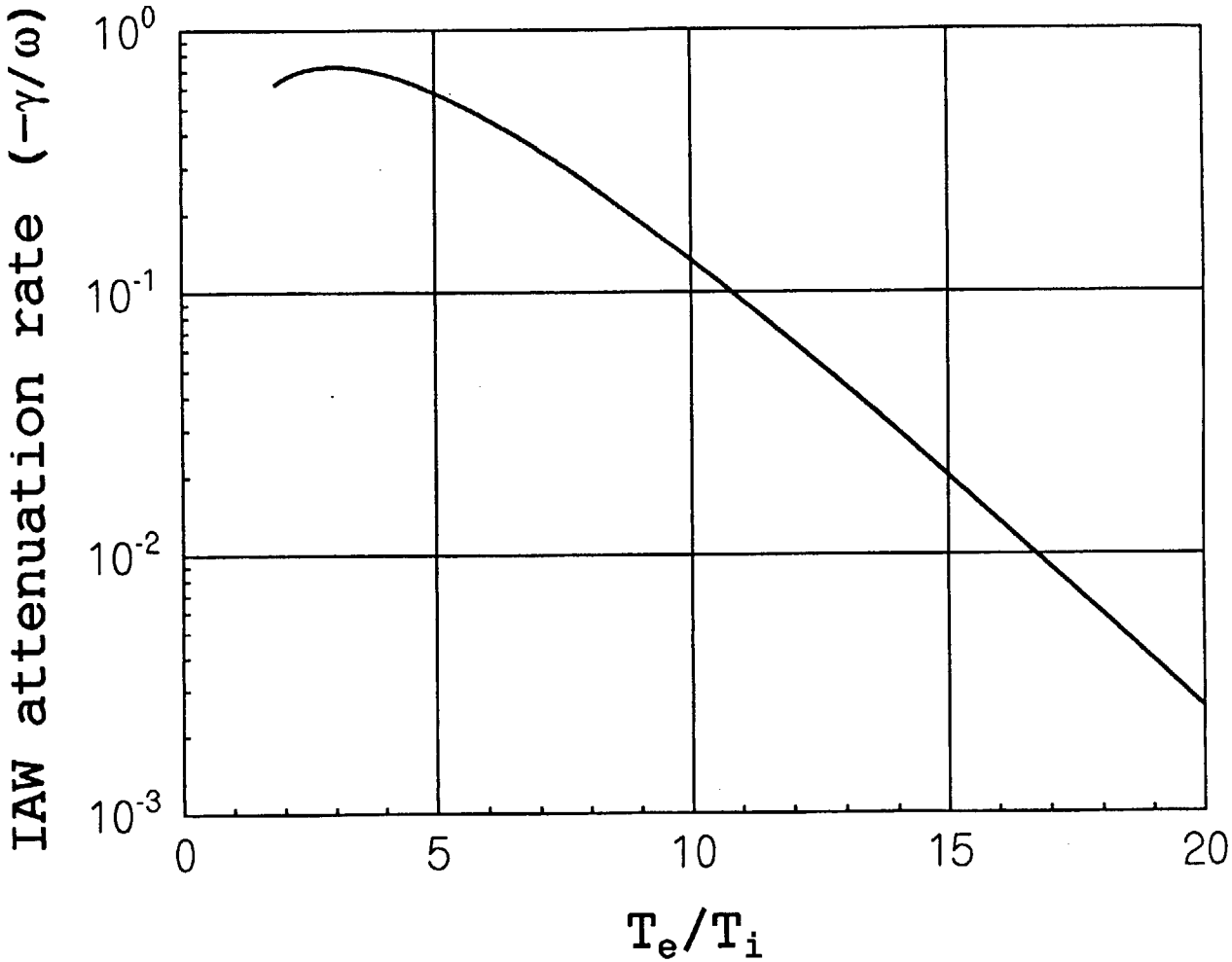

Fig. 11 The IAW attenuation rate vs. the ratio of electron and ion temperatures.

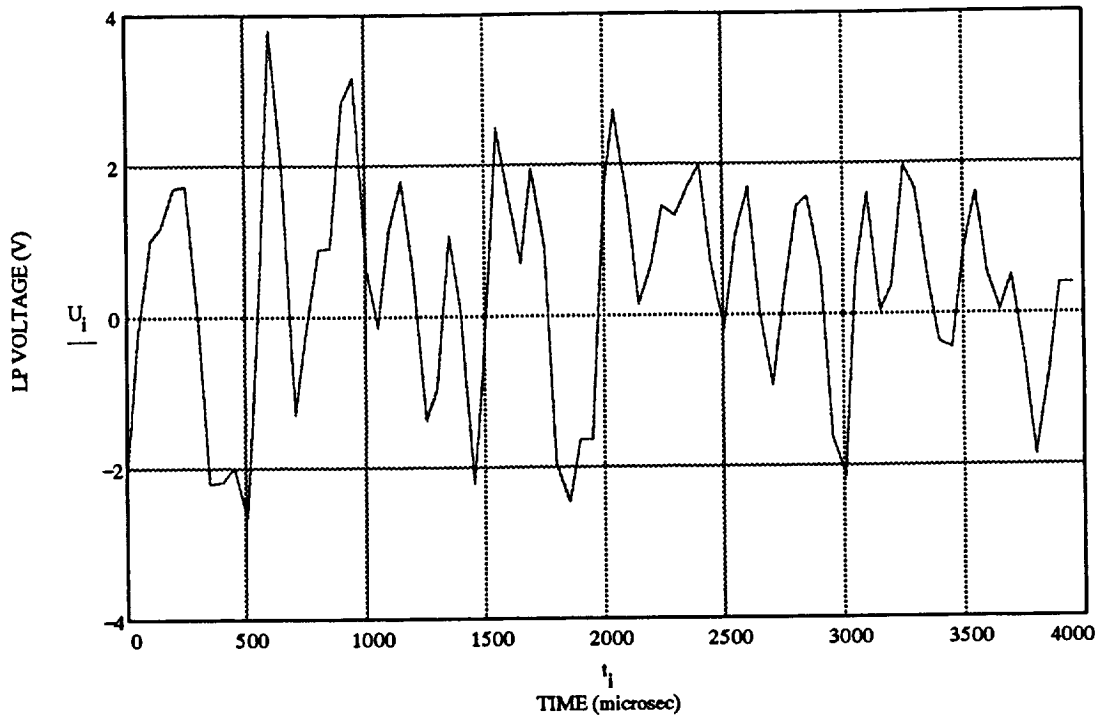

Fig. 12a. **LP output voltage fluctuations measured during the dwell in ram conditions when arcing occurred (MET 7/17:21). This plot demonstrates the large amplitude caused by arcing.**

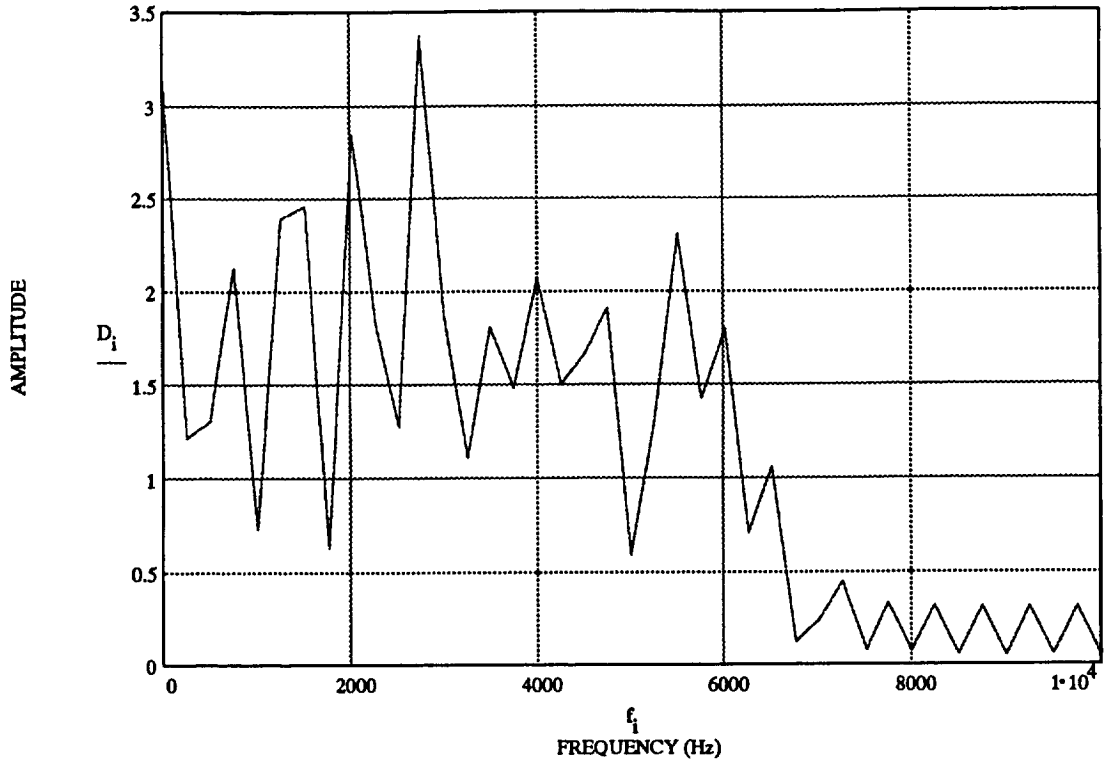

Fig. 12b The spectrum of signal shown in Fig. 12a

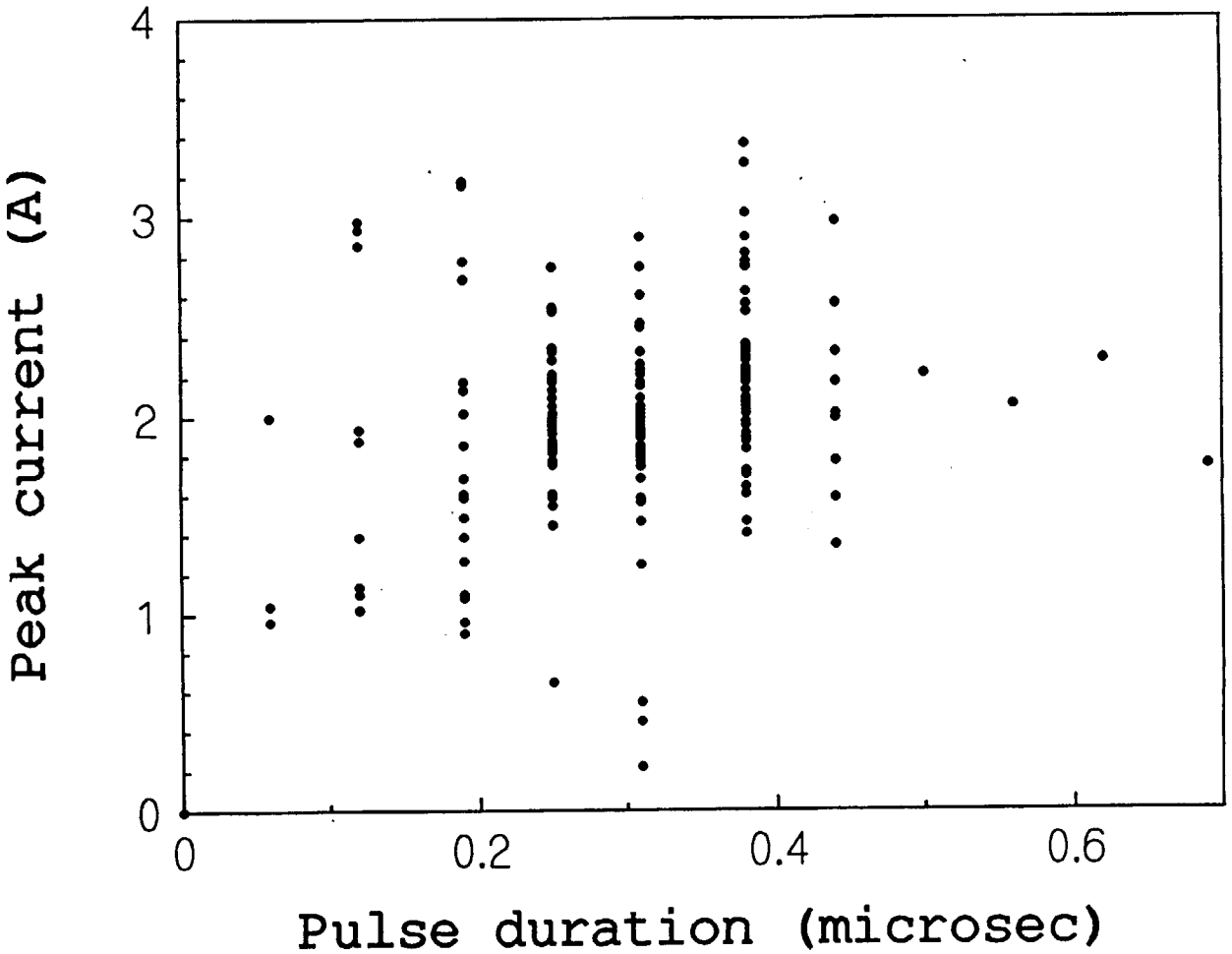

Fig. 13 Data from the Experiment #60-1/01. The bias voltage V=-400V, and 181 arcs were registered.

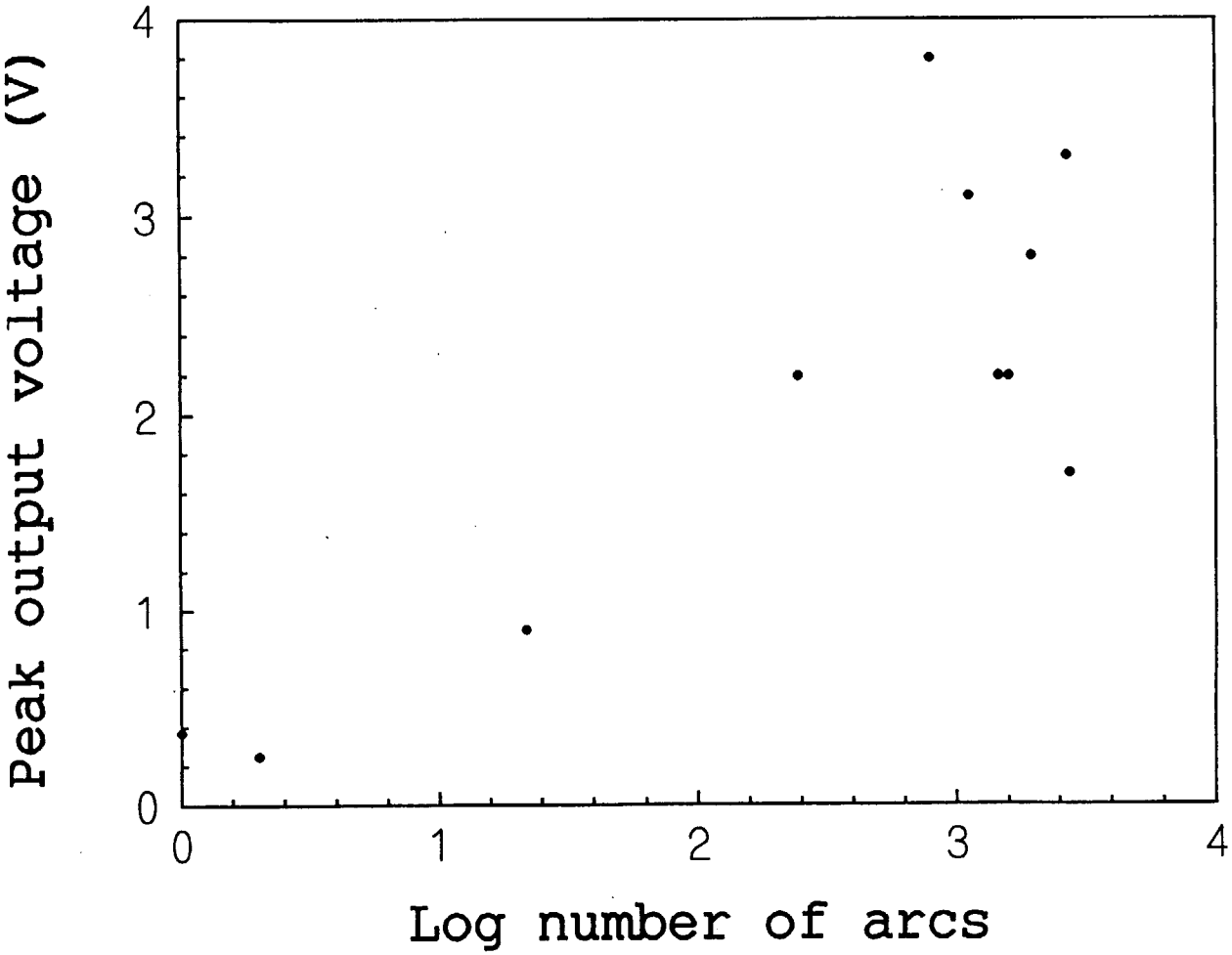

Fig. 14 LP peak voltage vs. the number of arcs per one experiment. Twelve dwells are used to draw this chart. No correlations were found between the peak voltage and the distance of the LP from biased solar cell samples.

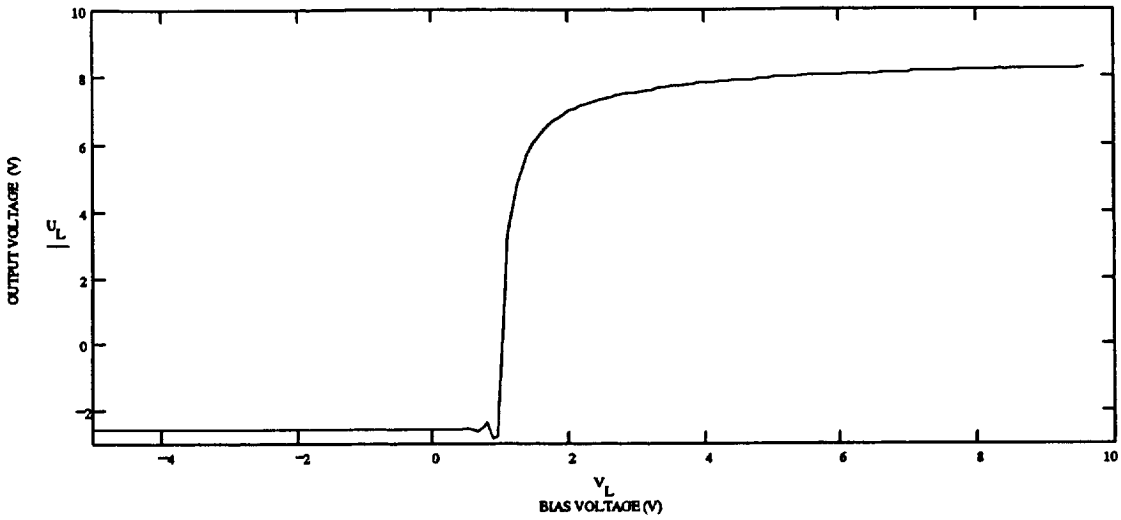

Fig.15. Langmuir characteristic for density $n_e=10^6$ cm^{-3}

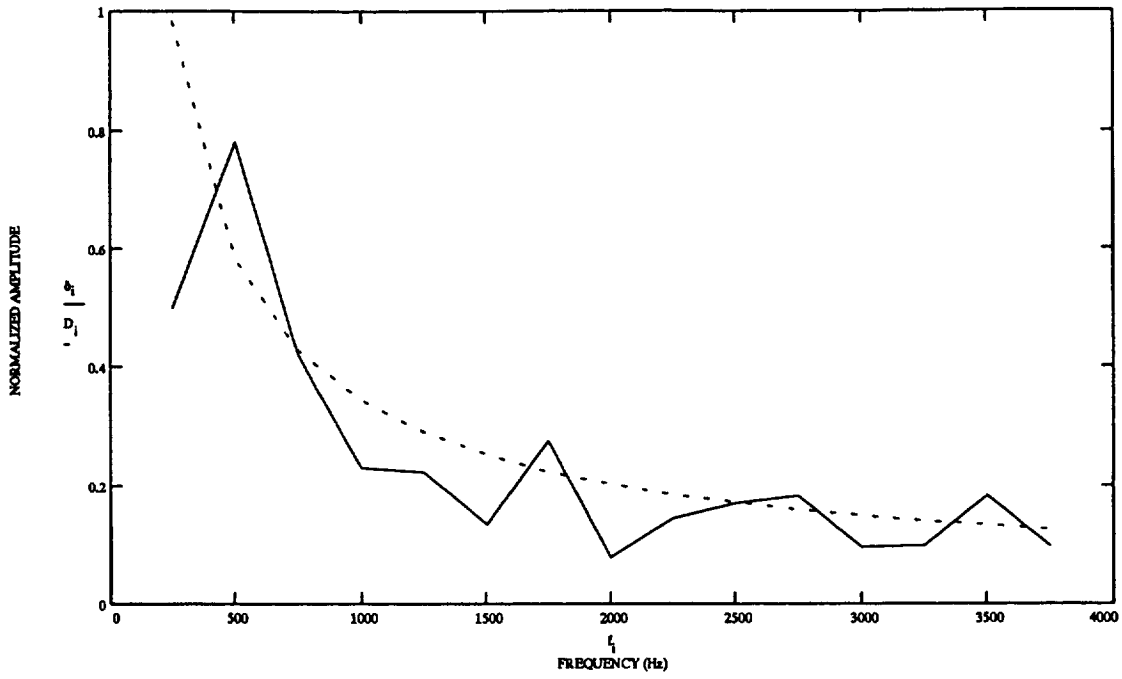

Fig.16a. Average spectrum that was built by using data from twelve dwells. The best fit approximation $D \propto f^{0.76\pm0.2}$ is in good agreement with theoretical predictions.

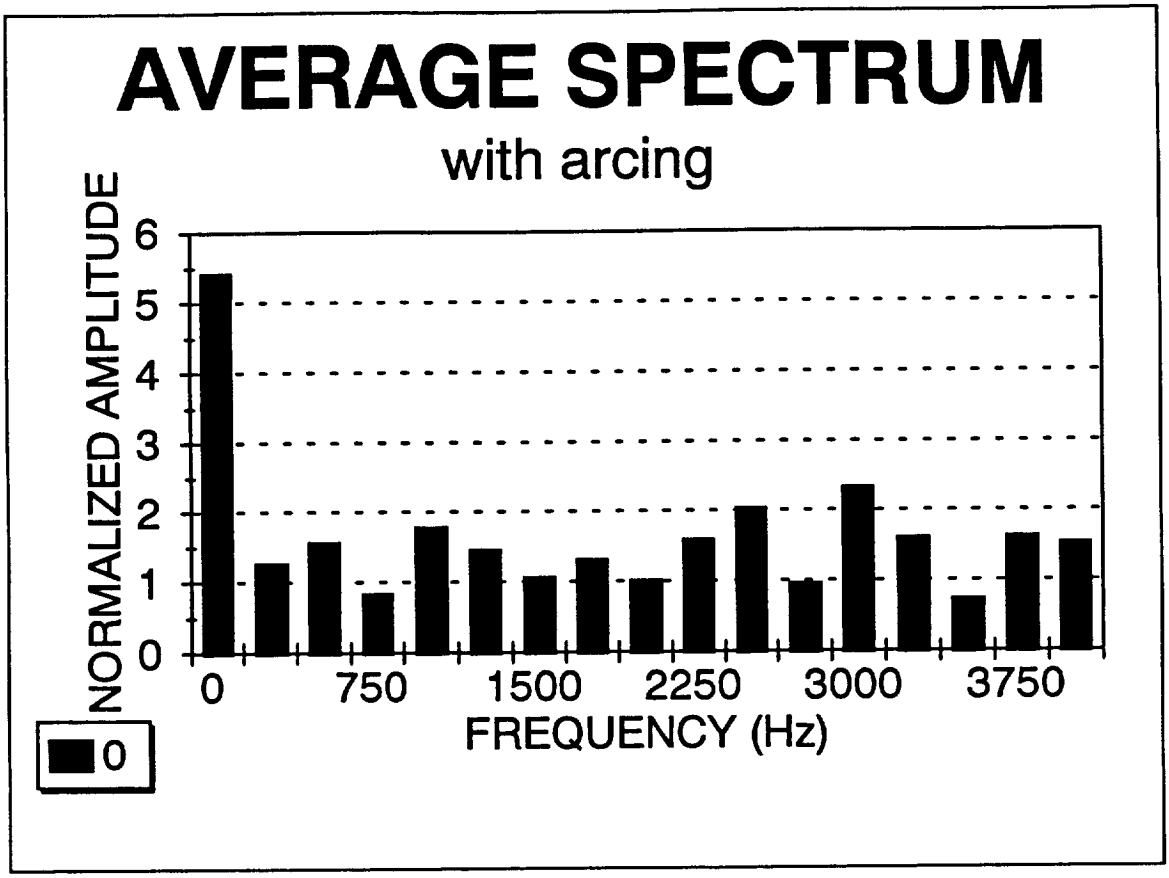

Fig. 16b Average spectrum that was build by using twelve dwells with arcing. It is seen that spectrum is almost flat for entire frequency range.

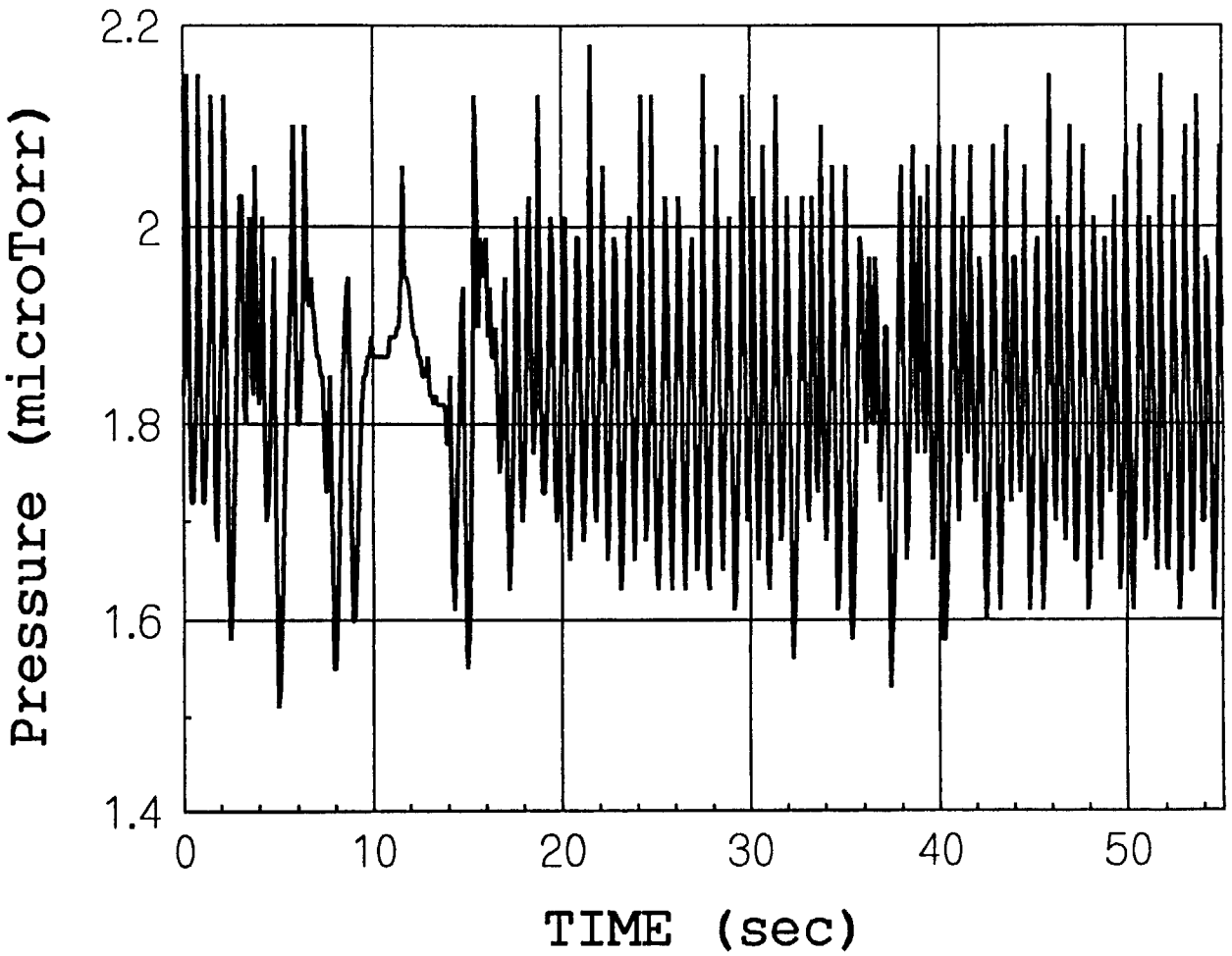

Fig. 17 The neutral gas pressure vs. time started at MET 7/16:04:18 (E_48-1/01)